BIOMIMETIC ADHESION FOR TRANSFER PRINTING VIA MICROSTRUCTURED SURFACES

BY

ANTON KOVALSKY

THESIS

Submitted in partial fulfillment of the requirements
for the degree of Master of Science in Materials Science and Engineering
in the Graduate College in the
University of Illinois at Urbana-Champaign, 2011

Urbana, Illinois

Adviser:

Professor John A. Rogers

ABSTRACT

Demand for robust engineering techniques on the micro and nano scales has been steadily growing in the age of modern technology, not only because of the driving force to fit electronics into smaller form factors, but also for a variety of other applications, from devices with microfluidic functions to components whose interfacial behaviors are key features. In our research we attempted to develop a tool that facilitates assembly of a wide variety of devices on both conventional and novel surfaces in the hopes of both improving modern capabilities of technological fabrication, as well as opening up possibilities for new classes of devices that can be easily assembled on surfaces and in form factors that were not previously possible. In summary, primary benefit of this technology is the potential ability to fabricate a variety of electronic devices on any surface – thus expanding the versatility and ability to integrate different classes of technology in way that is not possible using modern, competing fabrication methods for micro and nano-scale chemical/electronic/mechanical devices.

In the first two chapters, I will discuss background information relating to the basis and motivation for this technology, beginning with a summary of adhesion – how different types of adhesion occur and what their applicability is, with a focus on dispersive, or van der Waals adhesion – followed by a discussion of the field of biomimetics and how the study of naturally occurring dry adhesion techniques employed by animals such as geckos and insects has inspired a field of research into the use of dispersive intermolecular forces as an engineering solution for limitations of nanofabrication and assembly.

In the following chapters I will describe our own group's design, fabrication, and

testing of a variety of microstructured surfaces intended to control adhesive strength by increasing it and decreasing it, as needed.

Finally, I will present the results of our experiments and draw conclusions about the effectiveness and future potential of transfer printing via kinetically controlled microstructured stamps.

ACKNOWLEDGEMENTS

First and foremost, I would like to thank my adviser, Professor John A. Rogers. Professor Rogers provided limitless opportunities for my education, both by helping me personally to develop my ideas, and by cultivating the unique and fast-paced dynamic that his group is known for. I am very grateful to Professor Rogers for his support, which allowed me to contribute to the design and development of such a novel class of technologies. Furthermore, Professor Rogers' vision for the enormous potential of the projects I was fortunate to take part was truly inspiring for me. Above all, I hope to take with me what I learned from Professor Rogers' multifaceted approach to problem solving – with an equal focus on robust engineering and fabrication as well as the practical functionality of the end product.

I would like to thank all members of the Rogers group for the help they provided me in the form of time, effort, and advice. I would especially like to thank Andrew Carlson for the enormous amount of time and effort that he graciously spent helping me get trained, develop and present my ideas, and generally find my way through all of the work I had the pleasure of completing here. I would also like to thank Dr. Seok Kim for the leadership he provided on some of our most successful work. Thanks also to Matt Sykes for helping me to get settled into the project that would lead me to the bulk of my research.

Finally, I would like to thank the incredibly helpful individuals working in the Frederick Seitz Materials Research Laboratory and at the Beckman Institute – in particular Bharat Sankaran, Mike Marshall and Tony Banks at MRL, Scott Robinson in the microscopy suite at Beckman, and Darren Stevenson in the Imaging Technology group at Becman –

for the invaluable services the provided through training and advice on the various techniques used for my research.

TABLE OF CONTENTS

CHAPTER 1

ADHESIVE FORCES

Adhesion is the tendency of dissimilar particles and/or surfaces to cling to one another and cohesion refers to the tendency of similar or identical particles/surfaces to cling to one another [8]. The forces that cause adhesion and cohesion can be divided into several different types. The intermolecular forces responsible for the function of various kinds of adhesive devices fall mainly into the categories of chemical adhesion, diffusive adhesion and dispersive adhesion, also termed dry adhesion [8-12]. In addition to the cumulative magnitudes of these intermolecular forces, there are certain emergent mechanical effects that will also be discussed at the end of the chapter.

Adhesion is defined by surface energy and interfacial tension [8]. Surface energy is defined as the work that is required to build a unit area of a particular surface. From another perspective, the surface energy is the work required to cleave a bulk sample, creating two surfaces. If the new surfaces are identical, the surface energy γ of each surface is equal to half the work of cleavage, W:

$$\gamma = (1/2)W_{11}$$

If the surfaces are unequal, the Dupré equation applies:

$$W_{12} = \gamma_1 + \gamma_2 - \gamma_{12}$$

where γ_1 and γ_2 are the surface energies of the two new surfaces, and γ_{12} is the interfacial tension [8].

We can also use this methodology to discuss cleavage that happens in another medium:

$$\gamma_{12} = (1/2)W_{121} = (1/2)W_{212}.$$

These two energy quantities refer to the energy that is needed to cleave one species into two pieces while it is contained in a medium of the other species. Likewise for a three species system:

$$\gamma_{13} + \gamma_{23} - \gamma_{12} = W_{12} + W_{33} - W_{13} - W_{23} = W_{132},$$

where W_{132} is the energy of cleaving species 1 from species 2 in a medium of species 3 [8].

Chemical adhesion occurs when the surface atoms of two separate surfaces form ionic, covalent, or hydrogen bonds [8-10]. These attractive ionic and covalent forces are effective over only very small distances – less than a nanometer. This means in general not only that surfaces with the potential for chemical bonding need to be brought very close together, but also that these bonds are fairly brittle, since the surfaces then need to be *kept* close together. This is the most common type of artificial adhesion seen on a day-to-day basis. Glues, sticky tapes, and other such tools simply take advantage of chemicals that are reactive with common surfaces in appropriate ways.

Diffusive bonding occurs when species from one surface penetrate into an adjacent surface while still being bound to the phase of their surface of origin [9-12]. For example, diffusive bonding in polymer-on-polymer surfaces is the result of sections of polymer chains from one surface interdigitating with those of an adjacent surface. The freedom of movement of the polymers has a strong effect on their ability to interdigitate. Therefore, cross-linked polymers are less capable of diffusion and interdigitation because

they are bonded together at many points of contact, and are not free to twist into the adjacent surface. Uncross-linked polymers, on the other hand are freer to wander into the adjacent phase by extending tails and loops across the interface. Bonds such as these are also fairly common. They tend to be more permanent, and are often used in applications where separate objects need to be permanently fused together, for instance in the sintering of ceramic particles.

While the practical advantages of these types of adhesion are very clear – they are simple to use and can be very strong – they are not viable solutions to the problems facing those who wish to fabricate nanotechnological structures. Chemical adhesives tend to leave residue, not to mention the fact that they do not retain their adhesive nature, and the chemical adhesive must be replenished or replaced [8-10]. Diffusive bonding can only happen in situations where there is sufficient driving force for diffusion, and exhibits considerable hysteresis – that is, the adhesive capabilities change considerably with every time the bond is broken [9-12].

Nanotechnologists seeking to use adhesion as a locomotive to easily place the building blocks of their structures onto target substrates need a form of adhesion which is weak enough to be reversible, sturdy enough to be precise, and does not leave any residue that would interfere with the building or function of the device. This form of adhesion is also sometimes referred to as dry adhesion, due to the absence of covalent, ionic, and hydrogen bonding.

Nanotechnologists are attempting to address the need for clean, effective adhesive transportation of building materials via the use of a type bonding that arises from the van der Waals force, also called a London dispersive force. Described in the 1930s by Fritz London, dispersive forces are a consequence of statistical quantum mechanics [13]. London theorized that attractive forces between molecules which cannot be explained by ionic or covalent interaction, may be caused by transient polar moments within molecules. Multipoles could account for attraction between molecules having permanent multipole moments that participate in electrostatic interaction, but unfortunately, experimental data showed that many of the compounds observed to experience van der Waals forces had no multipoles at all. London suggested that momentary dipoles are induced purely by virtue of molecules being in proximity to one another. By solving the quantum mechanical system of two electrons as harmonic oscillators at some finite distance from one another, being displaced about their respective rest positions and interacting with each other's fields, London showed that the energy of this system is given by:

$$E = 3h\nu - \frac{3(h\nu\ \alpha^{2})}{4\quad R^{6}}$$

While the first term is simply the zero-point energy, the negative second term describes an attractive force between neighboring oscillators. The same argument can also be extended to a large number of coupled oscillators, and thus skirts issues that would negate the large scale attractive effects of permanent dipoles; cancelling through symmetry, in particular. The additive nature of the dispersion effect has another useful consequence. Consider a single such dispersive dipole, referred to as the origin dipole.

Since any origin dipole is inherently oriented so as to be attracted to the adjacent dipoles it induces, while the other, more distant dipoles are not correlated with the original dipole by any phase relation (thus on average contributing nothing), there is a net attractive force in a bulk of such particles. So not only is this form of adhesion useful in that it requires no chemical surfactant, but it does not even require the surfaces involved to be polar, making it any method employing dispersive adhesion all the more versatile [13].

When discussing adhesion, this theory needs to be converted into terms relating to surfaces. If there is a net attractive energy of cohesion in a bulk of similar molecules, then cleaving this bulk to produce two surfaces will yield surfaces with a dispersive surface energy. This theory provides a basis for the existence of van der Waals forces at the surface, which exist between any molecules having electrons. These forces are observed through the spontaneous jumping of smooth surfaces into contact. In the earliest studies performed by Derjaguin and Abrikosova in the 1950s, spontaneous jumping into contact was investigated for polished silica lens surfaces and it was shown that as the gap between the surfaces narrowed there was a rapid increase in adhesive attraction (reviewed by [9, 14]). However, since in these experiments the surfaces were too rough to allow decreasing the gap below 100 nm, the attraction remained relatively weak. In later experiments, Tabor and Winterton [15] showed that smooth surfaces of mica, gold, various polymers and solid gelatin solutions do not stay apart when their separating becomes small enough – on the order of 1-10 nm (reviewed by [9]). This behavior was predicted by the equation describing the attractive force between crossed cylinders that was derived in the 1930s by De Boer and Hamaker

$$P = -AD/12\ z^2$$

Where P is the force (negative for attraction), z is the separation distance, D is the diameter, z is the gap separating the surfaces of the cylinders, and A is a material specific constant called the Hamaker constant [9]. It is important to note that surface attraction forces depend on the geometry of the rigid objects and separate equations were derived for other geometries, such as two spheres or two flat surfaces [9, 16]

The effect of surfaces spontaneously jumping together is also apparent in experiments where a Polydimethylsiloxane (PDMS) stamp is made with small periodic post structures. The surface with the posts is placed face down on a smooth surface, such that the surface area in between each post is elevated above the smooth surface, like a roof supported by columns. Because of these attractive dispersive forces between the PDMS and the smooth substrate, the elevated surface – or "roof" – collapses down onto the substrate without any external force aside from the van der Waals attraction [3, 17]. It is important to note that such attractive forces also act over very small distances. 99% of the work necessary to break van der Waals bonds is done once surfaces are pulled more than a nanometer apart [9]. As a result of this limited motion in both the van der Waals and ionic/covalent bonding situations, practical effectiveness of adhesion due to either or both of these interactions leaves much to be desired. Once a crack begins, it propagates easily along the interface because of the brittle nature of the interfacial bonds [18].

As an additional consequence, increasing surface area often does little to enhance the ultimate strength of the bond in this situation. This follows from the aforementioned

crack failure – the stress at the interface is not uniformly distributed, but rather concentrated at the area of failure [9].

Simple smooth polymer surfaces – without any microstructures – are commonly used for these dispersive adhesive properties. Decals and stickers that adhere to glass without using any chemical adhesives are fairly common as toys and decorations and useful as removable labels because they do not rapidly lose their adhesive properties, as do sticky tapes that use adhesive chemical compounds. However, while dispersive adhesion enables us to temporarily bind surfaces together with little to no hysteresis, but to really achieve the levels of versatility and dexterity necessary to utilize dry adhesion in a technological approach to nanofabrication, we must figure out a way to more finely control this adhesion.

In nature, dry adhesion is very common on the microscopic scale. It is apparent in many systems, from the ability of various animals to adhere to almost any surface, to the adhesive capabilities of certain parts of some plants for the purposes of pollenation. Researchers have long looked to these examples to better understand the potential of this sort of adhesive action, and more recently have begun to apply their conclusions to new technologies.

CHAPTER 2

BIOMIMETICS & INSPIRATION FOR TRANSFER PRINTING

Biomemetics is the concept of applying naturally occurring, evolved "technologies" to artificial engineering, such as water resistant glues based on mussel adhesive [19], strain gauging based on receptors of insects [20] and generation of novel adhesive surfaces based on the fibrillar structures found on the feet of insects and some amphibians [21], also reviewed by [5, 22].

The microstructures that enable creatures such as spiders and geckos to cling to surfaces function as a versatile adhesive, capable of withstanding relatively high loads [5]. The advantages of using such a design in engineering applications stem from the fact that these functions depend more so on form factor than on surface chemistry [23, 24].

The role of van der Waals forces. Multiple studies have addressed the question of what sort of adhesion geckos are using that allows them to run on vertical and inverted surfaces (reviewed by [5, 24]. Two competing hypotheses have been proposed: (i) thin-film capillary forces or some other mechanism relying on hydrophilic action, which indeed are known to contribute to adhesion in insects and frogs (e.g. [25, 26]) or (ii) dispersive van der Waals attraction. In geckos, while a granular secretion of a glue-like substance could be ruled out, as geckos do not possess such skin glans at their feet [23, 24, 27], thin-film capillary adhesion could still play a role due to possible absorption of water from the atmosphere [23]. To discriminate between these possibilities, Autumn et al (2000) [28] measured the adhesive and shear force of a single isolated gecko setae

using micro-electromechanical systems force sensor that allows independent detection of vertical and lateral forces, a method developed by Chui et al (1998) [29]. The authors suggested that these data provide an indirect evidence for the van der Waals adhesion being primarily responsible for the adhesive action in this system. Moreover, the authors also pointed out that these data do not support neither suction nor friction as the major mechanisms for the adhesion in this system because (a) measurements of greater than atmospheric pressure adhesion indicate that suction is not the primary source of adhesion, and (b) adhesion due to frictional effects is also unlikely since the friction coefficient between the setal keratin on silicon is low (μ=0.25). It is also important to note that very early experiments performed by Schmidt in the beginning of the twentieth century demonstrated that the setae maintain their adhesive properties in ionized air suggesting that electrostatic attraction is not involved [28].

Finally, a more recent study of Autumn et al (2002) [23] provided the most direct evidence to rule out the possibility that capillary action contributes significantly to the adhesion of gecho setae. In this study, Autumn et al compared the adhesion of gecko foot pads to polarizable semiconductor surfaces that were either hydrophobic or hydrophilic [23]. The study showed that adhesion was comparable on the highly hydrophobic GaAs (contact angle = 110 degrees) surface and the highly hydrophilic surface SiO2 (contact angle = 0). These observations are incompatible with the capillary forces hypothesis because if indeed capillary forces were responsible for the gecko's adhesive capability, this adhesion would have been reduced on the hydrophobic surface in comparison with the hydrophilic one. It is also worth noting that setae do not adhere strongly to surfaces

that are weakly polarizable, such as polytetraflouroethylene (dielectric constant ε=2.0) [23]. The polarizability of a surface would have an effect with either dispersive or capillary adhesion, as London dispersion does depend on the ability of a surface to experience at least momentary dipoles, so the experimental data is consistent with the conclusion of dispersive forces as the source of adhesive action. Taken together, these studies point to va der Waals forces being the primary contributor to gecko adhesion.

Having identified the intermolecular forces responsible for the dry adhesion we wish to take advantage of, we must now explore the effects of various form factors on this action. Dispersive adhesion is an ideal solution to many challenges of nanofabrication because it can occur between two surfaces of almost any type. However, to modulate the exact strength of this adhesion, nature has evolved a variety of physical form factors that allow the gecko to both increase and decrease the strength of its adhesive action as needed.

One example of a basic feature found in nature is contact splitting. The pads of a gecko's foot are covered by complex hierarchical structures that enable it not only to stick to several types of surfaces, but also to be able to unstick itself with ease, and to do so over an indefinite amount of cycles. The pads on the foot of a gecko are covered with microscopic hairs, each of which in turn splits into hundreds of smaller tips. More specifically, the foot of a tokay gecko bears approximately 14,400 setae per mm^2 with the total number of septae per animal approaching 6.5 million [24, 30]. This form factor produces an enormous increase in the potential strength of the bond a gecko can make with most surfaces.

Johnson-Kendall-Roberts (JKR) theory is a theory that models the energy balance between contacting spheres [31]. This model predicts a theoretical adhesive force (Fc) for a sphere in contact with a plane:

$$Fc = (3/2)\pi * R * \gamma$$

where R is the sphere's radius and γ is the work of adhesion.

Applying this model to living systems, Arzt et al (2003) developed the "contact splitting" principle a phenomenon in which the terminal contacting surface of an adhesive device or limb is split into multiple branches [2, 32]. In this way the adhesive strength of such a surface, often referred to as a fibrillar surface, is significantly greater than that of a flat surface with acomparable surface area. Based on this principle, the strength of the bond increases by a factor of $n^{1/2}$, as one large spherical contact is subdivided into n smaller contacts with the identical apparent contact area [2]. Indeed, we can try to increase the strength of this bond by a factor of n in two ways: we can make n number of spheres of radius R contact the plane, or we can increase the radius by a factor of n. Since the interfacial contact area in all cases is circular, however, in the latter case the contact area increases by a factor of n^2, while in the former case the increase is only by a factor of n. If we reverse this logic, stating that we wish to compare equivalent total contact areas, we can see that increasing the number of contact elements causes a greater increase in adhesive force than just increasing the size of a single contact element. To be specific, as described above, when a contact is subdivided into n smaller elements with an equivalent total contact area, the adhesive force increases by a factor of n^(1/2) [2].

In nature, this phenomenon is expressed by the fact that the heavier the animal is,

the more subdivided the fibrillar structures on their foot pads [2]. This principle is illustrated in **Figure 1** showing that the heavier the creature, the greater hierarchical complexity and thus the greater amount of contact elements. For instance, geckos have much more and much finer contact elements than do insects. Contact splitting is a highly effective method for the improvement of adhesive abilities because it is the source of multiple effects that serve to increase the integrity of an interfacial bond. The aforementioned consequence of JKR theory explains how contact splitting, coupled with an optimized area density of contact elements produces a higher maximum potential adhesive force. In addition, fibrillar surfaces exhibit a lower effective elastic Young's modulus than do planar surfaces, and as a result of their ability to deform, are able to make much more conformal contact with rough surfaces [33]. In this way, animals take advantage not only of the aforementioned consequences of JKR theory to increase the potential maximum of their adhesive capabilities, but also of improved conformal contact to rough surfaces, thus maximizing their ability to reach this full potential.

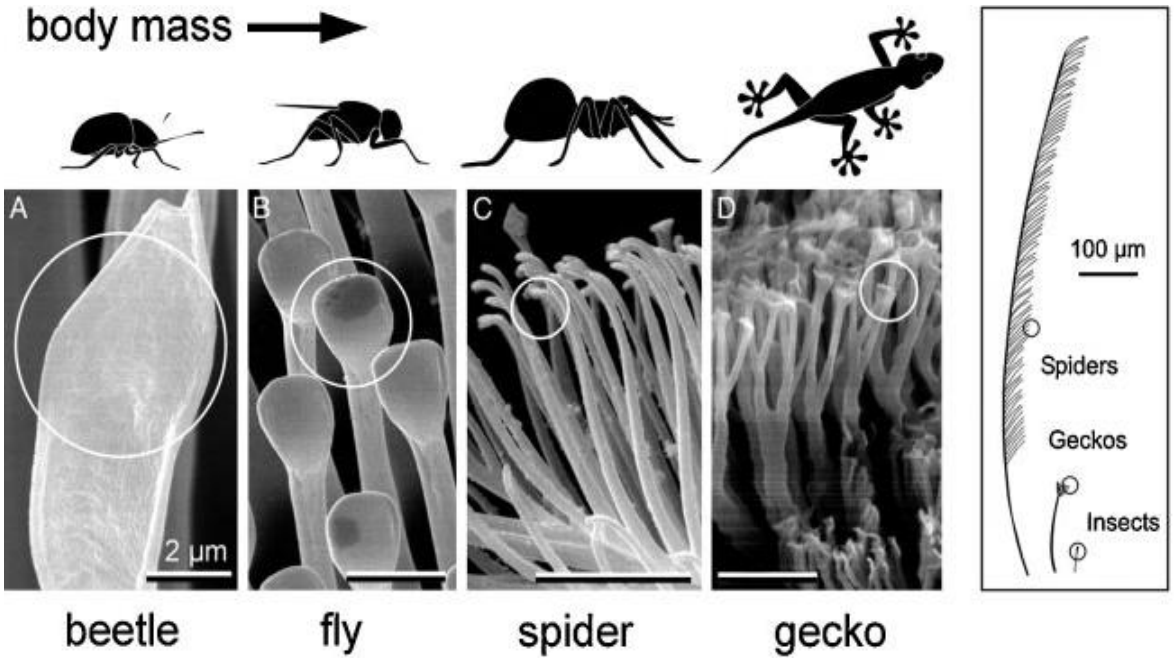

Figure 1. Contact splitting of foot hairs on animals with hairy attachment pads. Note that contact splitting hierarchically increases in fineness of contact elements (from left to right) as animal size increases. The rightmost panel shows a close-up schematic of the individual setae of each animal [2].

On top of those effects, the gecko also benefits from the crack arresting properties inherent to this form factor [32]. In order for this interfacial bond to fail, the load it experiences must be great enough to initiate failure at every contact, and must be sustained long enough. Otherwise, if only a few contacts are broken, once the load is removed, they may collapse right back onto the substrate in much the same way that roof collapse occurs in PDMS, as described earlier.

Another example of a naturally occurring form factor that inherently strengthens these abilities is the shape of individual setae. Gecko toe pad fibers are spatula shaped, and thus distribute stress at the interface in a way that facilitates a higher pull-off force necessary

to break the bond [28, 34]. This effect will be described in more detail in the chapter on microstructures. In essence, stress is concentrated at the center of the interface, rather than around the perimeter, where crack initiation would normally occur.

Ultimately, research aimed at mimicking the adhesive capabilities of biological systems provides inspiration for technologies that benefit from various aspects of these systems. Understanding details such as how contact splitting enhances adhesion strength, or how van der Waals forces enable dry adhesion to most types of surfaces provides opportunities for creative solutions to engineering problems in which surface reactivity, contaminants, or strength of adhesion present significant obstacles.

While initial interest in naturally occurring adhesion stemmed from the surprising level of strength and versatility that such bonds could provide without the use of complex chemistry, it is the reversibility and reusability of this system that provides the inspiration for its use in the technological application of transfer printing; the focus of this thesis (**Figure 2**).

Transfer printing is a method by which micro and nanoscopic samples of different materials may be manipulated and relocated for a variety of uses [4, 35, 36]. Multiple devices can benefit from this method of fabrication including computer chips, microfluidic devices such as lab-on-a-chip technologies currently in development [37], nanotube devices [38], cantilevers [39], and LED devices [40, 41]. One of the most attractive advantages of this technology is the ability to transfer semiconductor materials from their growth substrates to many other types of surfaces, such as silicon, glass,

plastic, paper and rubber [36]. This capability allows for the integration of electronic devices into a variety of systems such as biological systems, hemispherical "eyeball" imagers, flexible displays and lighting devices, and photovoltaic modules [36].

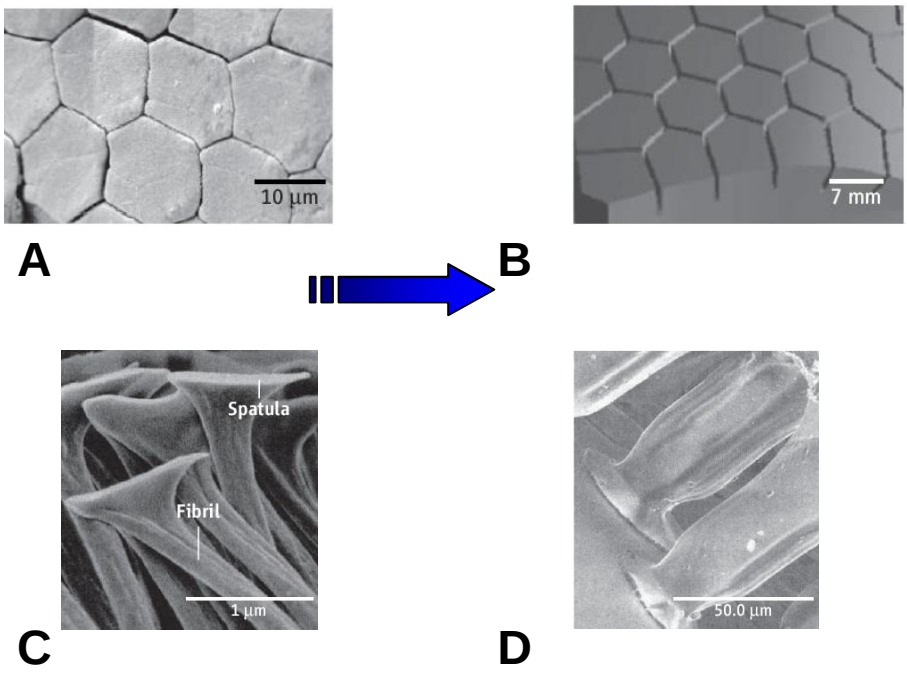

Figure 2. Biomimetically inspired artificial devices. Hexagonal toe pads of a tree frog (A) serve as inspiration for tire treads (B) because they offer better interfacial grip. Spatula shaped ends on the toe hairs of geckos (C) facilitate much stronger adhesion, making this form factor desirable for fibrillar surfaces used by climbing robots (D).

In addition to devices such as the ones mentioned above, researchers in the sciences and engineering have a general need for small scale fabrication techniques to create esoteric devices whose only purpose is to answer specific experimental questions. For example, researchers studying proximity effects of superconductivity need to deposit small islands of superconducting material onto graphene surfaces [42]. Currently, such research is facilitated by lithographic fabrication techniques, which are difficult because

of their relatively low sensitivity to small process flow details such as times of exposure to light sources, heating elements, or chemical baths, and the need for extremely clean environments.

There are several types of commonly used lithographic techniques such as photolithography and reactive ion etching (RIE) [7, 41, 43-46]. In these techniques, building material is deposited onto a substrate in layers, and then patterned using a reactive etching procedure. There are many different building materials and as many corresponding etching methods, each with its own advantages and disadvantages. In photolithography, a layer of photoresist is deposited evenly onto a substrate, covered with a mask bearing the desired pattern, and exposed to a dosage of UV light that is specific to that particular formulation and layer thickness of photoresist.,a polymer that is altered by UV exposure by becoming more basic, acidic, or neutral [44]. Depending on how the chemistry of the layer is altered, a chemical bath is chosen and the sample is placed in the bath so that some portions of the layer are developed away, while some remain. In reactive ion etching (RIE), instead of a chemical bath, the sample is placed in a chamber that is then filled with a gas of ionized atoms that are reactive with that layer. Rather than a transparent mask, the pattern must be provided by another layer on top of the target layer. In this way, RIE is used in conjunction with photolithography. Complicating things further is the fact that with all types of lithography, there is a plethora of pairings when it comes to building material layers – photoresists with opposite behaviors; different surfaces capable of reacting with ionized gases – and etching procedures. Each fabrication procedure must be carefully planned out to make sure that none of the steps

interfere in unfavorable ways with one another, and ultimately produce exactly the forms necessary. Making simple devices can require a variety of chemicals and large, expensive, difficult to operate and maintain pieces of equipment, such as spin coaters, mask aligners, etc.

Ironically, since the technology that may serve as a superior alternative to the methods described above is not yet available, lithography was the primary method used to fabricate the prototypes that will be discussed in this thesis. As such, a more detailed discussion of these methods and how they were used for this research will be included in the section on fabrication.

Although lithographic techniques provide a robust toolkit for the skilled user, transfer printing would be inherently better in most ways. Rather than depositing layers from which the necessary shapes must cut out, the user would be able to build the desired structures from basic building blocks, as if s/he were making a Lego model. Rather than needing a series of wildly different steps and pieces of equipment, the user would only need to load the substrate and a supply of the desired building blocks into the transfer printer. Rather than requiring a clean room environment, the user will be able to suffice with making certain the components are clean until they are loaded into the single machine necessary for the fabrication process. Rather than using a battery of chemicals to facilitate fabrication when those chemicals themselves may interfere with the device's function, the user can put the building blocks together manually.

Most importantly, the fabrication process would itself become conceptually simpler. Besides the highly demanding nature of lithography, its inherent complexity makes fabrication more difficult as the device being built gets more sophisticated. An item that is easy to visualize – and would therefore be easy to build out of simple blocks – may require a highly complex procedure, and can be extremely difficult or even impossible to fabricate successfully [47]. With transfer printing, the limitations would only arise from the dimensions of the building blocks themselves. Simply put, the greatest advantage that transfer printing would have over current nanofabrication techniques is that it is a bottom-up approach, while others are largely top-down approaches. A good analogy might be to say that lithography is much more difficult than transfer printing in the same way that shadow puppetry is more difficult than pencil drawing.

The ability to enhance strength of adhesion and the versatility and cleanliness of dispersive adhesion are clear advantages in any attempt to biomimetically implement this knowledge to create a machine that can effectively pick up building blocks for nanotechnological devices. However, the lynchpin that makes this technology possible is reversibility. Loading the building block onto some adhesive surface is a simple task, but in order for this technique to have any use, it is crucial that depositing the building block back down onto a target substrate be just as easy as it was to pick it up.

It is the gecko's ability to both stick and unstick itself with ease that makes a biomimetic solution to this problem seem likely. The reversibility of the gecko's adhesive

capabilities has also been the focus of much research (reviewed by [5]). How exactly the gecko accomplishes this feat is still unclear, but several mechanisms have been proposed, and evidence has been presented for each. These mechanisms can mainly be divided into two categories: The gecko may be altering the shape of the setae and/or the contact elements themselves at will, driving down a given foot's adhesion to a surface so that it may be lifted, or the gecko may be moving his foot in a particular fashion that facilitates the breaking of the bonds between the footpad and the substrate. Specifically, it has been theorized that the gecko is using some form of shear motion. Both methods of reversing the bond strength of a dry adhesive surface have been supported theoretically and experimentally by making biomimetic stamps and using each method to drive down the force necessary to break the bond [5]. Additionally, not only is it plausible that the gecko is using both methods in parallel, but that form factor and motion can be used in conjunction. Experimental data shows that coupling some directionality of form factor with directionality of motion yields effective results. Several groups have shown that angled nanohairs require different magnitudes of force to break their bonds with a target substrate, depending on the relation of the direction of that force to the direction of their angle. It has also been demonstrated that many form factors of non-fibrillar patterned surfaces require different amounts of force to peel them from target substrates depending on the direction of peeling, similarly to the way that treads experience higher traction in some directions.

Besides cleanliness, strength, and reversibility, biomimetic research has shown an encouraging level of reusability to these systems. Researchers studying geckos have

reported evidence that the gecko's adhesive pads exhibit self-cleaning capabilities [5]. The mechanism for this is unclear, but since the gecko does not use any natural secretion to do this, it is likely accomplished using some application of the aforementioned concepts. The gecko is able to minimize and reverse adhesion of foreign particulates to its footpads, and is thus able to maintain its adhesive abilities for thousands if not millions of cycles between molts. Meanwhile, researchers who fabricate dry adhesive fibrillar surfaces report that their samples retained adhesive capability for as many as 1,100 cycles.

Because all of these effects are observed specifically on the micro and nano scale, biomimetic research has made it clear that it is possible to complete all of the tasks necessary to cleanly transfer building materials from one substrate to another on a much smaller scale than could ever be done before. The focus of our research is to investigate the adhesive properties needed at that interface. Once it is clear how the dimensions of microstructures affect their adhesive capabilities, engineers can simply pick and choose microstructural form factors that optimize adhesive function for their application from a menu of two and three dimensional features. Several representative examples of the structural features which can be fabricated using available microfabrication techniques will be described in detail in the Microstructures chapter. Many of these features are directly inspired by the naturally occurring shapes that have developed to facilitate adhesion in the animal kingdom.

CHAPTER 3

FABRICATION

To make our samples, we start with a Silicon-on-Oxide (SOI) wafer, and use a variety of lithographic techniques to pattern the negative of our desired three dimensional shape onto the surface of the wafer. We then cast our samples in polydimethylsiloxane (PDMS) against the mold we built on our SOI wafer [7].

Lithography on the micro and nano scale is a method by which three dimensional structures are built layer by layer, where every layer of material is a coat with a controlled thickness which then has a two dimensional pattern etched into it [48]. **Figure 3** shows some examples of the level of detail achievable with these techniques. The techniques that comprise this method are differentiated primarily by the chemical makeup of the building layer and by the chemical process that facilitates the etching of a pattern into the layer. The layer of building material has its chemical makeup altered by heat treatment or exposure to light.

The most common lithographic technique employs a polymer called photo resist [7, 41, 45, 46]. Depending on the exact chemical properties of a given photo resist, UV exposure will cause bonds to break inside of the layer in such a way as to make it more acidic or more basic. The sample is then washed in a solution that is reactive with the treated material. This solution is alternately referred to as the etchant or the developer. By covering a coated sample with a transparent mask that has a pattern of dark spots on it, users can control which areas on the photo resist layer become more reactive, so that

when they wash their sample in etchant solution for an appropriate amount of time, a desired pattern will remain. Moreover, photoresists can either be negative tone or positive

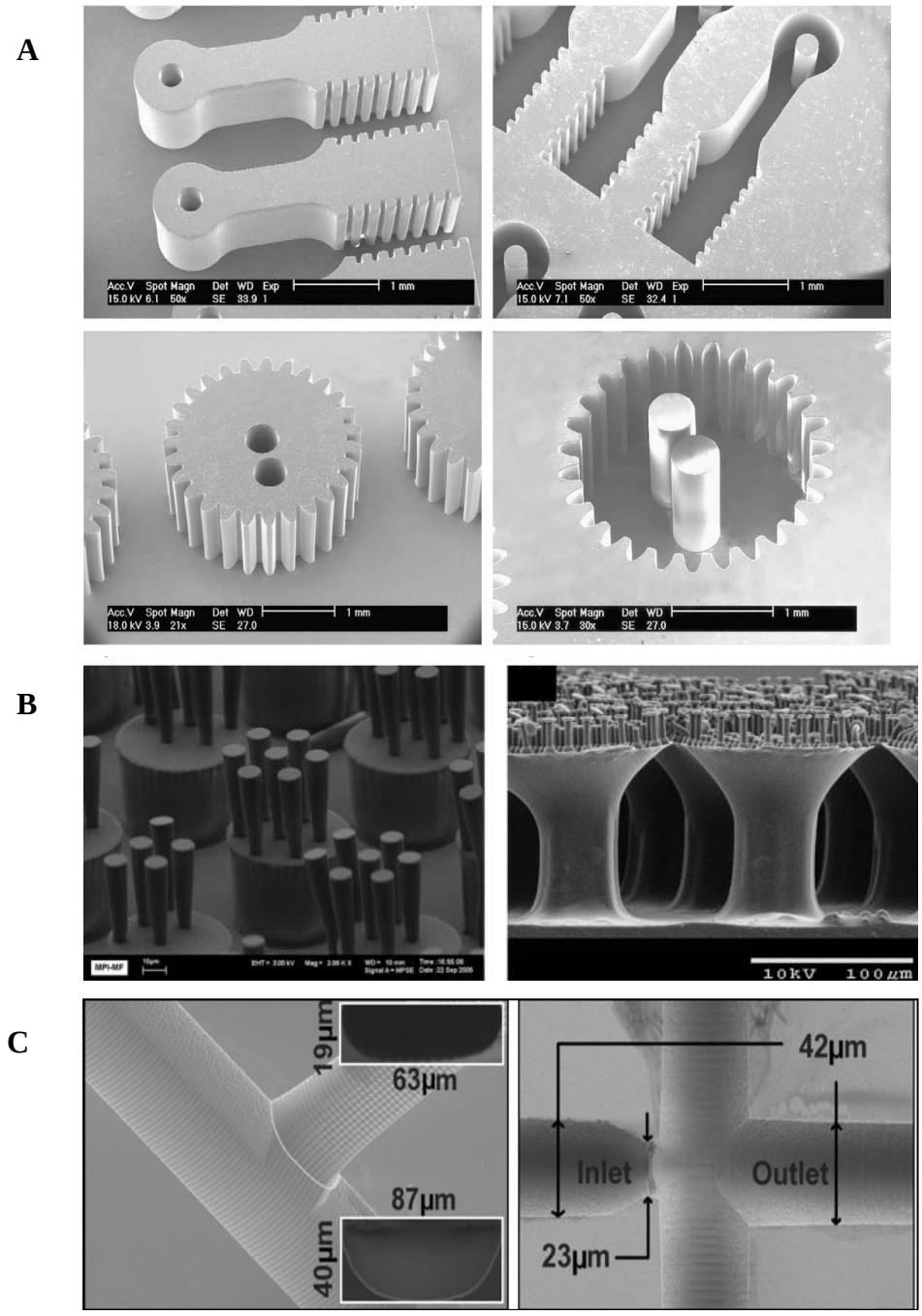

Figure 3: Examples of lithographically defined nanoscale devices. Gear type devices (A) [1], arrays of fibrillar surfaces (B) [5], microfluidic channels (C) [6].

tone. A positive tone photoresist becomes more soluble to its developer when it is exposed to light, while a negative tone photoresist becomes less soluble. So if a sample is covered with a patterned transparent mask and then flooded with a dosage of UV light, if it is a positive tone photo resist, the pattern on the mask will be the one remaining. If it is a negative tone resist, then the pattern appearing on the mask will be developed away at the end of the procedure, leaving its negative behind.

Photo resist lithography is referred to as photolithography, and while common, is not the only tool in the lithographic tool box. Reactive Ion Etching (RIE) is a procedure in which plasma ions attack the surface of a sample. The sample is placed in a low pressure chamber and a plasma of an appropriate ion species is generated by an electromagnetic field. RIE is a technique that functions in a line-of-sight mode, which is to say the plasma etches straight down in a direction normal to the surface that the plasma ions are impinging on. In order to pattern a surface coherently using RIE, it is necessary to pre-pattern it using photoresist. Because RIE works on a line-of-sight basis, it will not attack material that is directly underneath a layer of photoresist, but it will attack the surface directly adjacent to a feature patterned with photoresist. Thus, a layer of photoresist is patterned on a silicon wafer, the sample is placed in the RIE chamber, the pattern is etched into the underlying silicon layer by the plasma, at which point the photoresist may be washed away, leaving the same pattern transferred into the silicon. The advantage here is that now we have one level of features on our mold that is not made of photoresist. If we wish to make our mold more complex, we can perform another level of lithographic fabrication. Ultimately, combining different types of etching

procedures enables exponentially more complex samples to be fabricated.

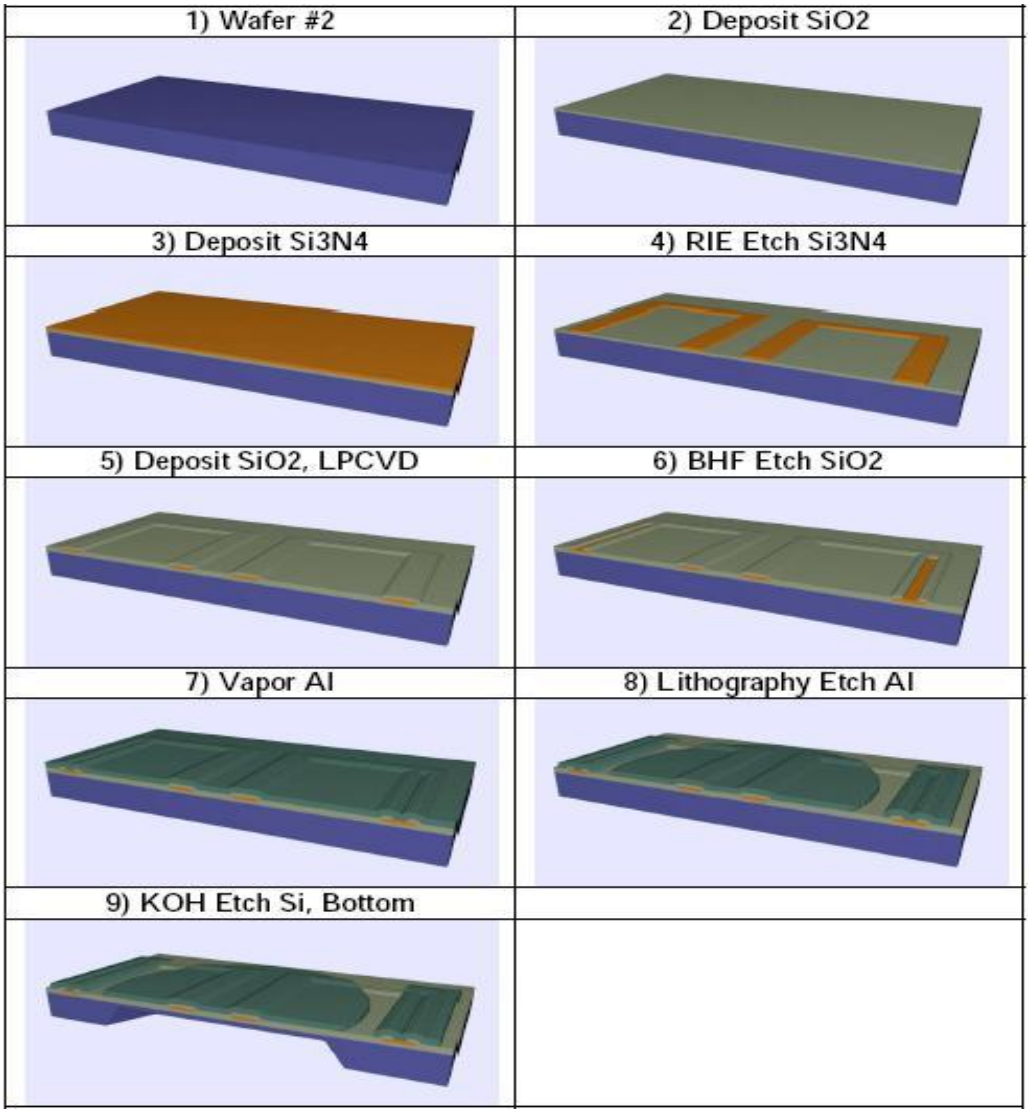

Figure 4. A process flow modeled in clean room modeling software. This figure demonstrates the complexity that is possible to achieve through the use of multistep lithography. The process flow shown is for the construction of a bimetallic membrane for a micro pump. Construction from photoresist is not conducive to the function of such a device, but is very useful for our purposes, which mainly involve the fabrication of molds for the structuring of elastomeric surfaces. http://intellisense.wordpress.com/category/academia/

Usually, each layer must be deposited and patterned before another layer is added, although there are a few cases in which multiple layers may be deposited, and then patterned one after the other [41]. An example of such a procedure is shown in **Figure 4** (http://intellisense.wordpress.com/category/academia/, Developing a microresonator in IntelliSuite).

Sometimes a stacked procedure like this will facilitate certain feature aspects. For instance, the phenomenon in which a chemical etchant is eating away at material that is sandwiched between two layers on which that etchant has no effect is called "undercutting", and is useful in making structures that have an overhanging feature. Undercutting is a consequence of isotropic etching – the etchant attacks the building material equally in all directions. Some lithographic etching reactions are isotropic, and some are anisotropic. An anisotropic etching process is yet another tool that can be selected for its specialized function. For instance, KOH etches through Silicon 100 at an angle of 54.74 degrees (**Figure 5**) (http://cleanroom.byu.edu/KOH.phtml, Department of Electrical and Computer engineering, Brigham Young University)). So if tapered walls are a desired feature, the user can design their process to include an anisotropic etching step.

Figure 5. Diagram of anisotropic etching of a SI[100] surface. The yellow layer represents a mask patterned over the gray layer of Silicon. Once the etchant begins etching the Si layer, it etches down at an angle of 54.74 degrees. Other anisotropic etching angles are achievable with surfaces of different atomic structure and/or orientation (http://cleanroom.byu.edu/KOH.phtml).

These methods are used to etch micro and nano scale three dimensional objects. In our research, these objects were not the final samples, but rather the molds in which the PDMS was cured [7]. So any shape we tested, we would have its negative made using photolithography, and then pour uncured PDMS onto the mold, and allow it to cure in an oven. PDMS is an organic polymer used in an enormous variety of applications, from medical devices to shampoos [49]. It is inert, non-flammable, non-toxic, and is notable for its viscoelastic properties. It is an ideal material for testing van der Waals adhesion because at room temperature and on the time scale of our experiments, it behaves as an elastic solid after it has been cured with an agent that catalyzes cross-linking. The conditions of this curing process – the amount of catalyst, and the temperature and duration of the curing process – control the elastic modulus of the finished sample. Elasticity facilitates conformal contact, which is key to the function of dry adhesion, and such a versatile elastomer kit provides us with the ability to test the effects of different levels of elasticity on adhesive function. We used a standard kit, SYLGARD 184, which provided ten parts polymer to one part catalyst. This formulation produced a resin with an elastic modulus of approximately 2.8 MPa [3], but we occasionally mixed in twice as much catalyst (a 5:1 solution) to make a sample that was twice as stiff [7]. PDMS is also relatively non-reactive and hydrophobic, which is advantageous to the measurement of adhesion due to van der Waals forces, as it eliminates most possible false positives. In our experiments, the only force that interfered with our measurements was an electric force caused by static charge build up over repeated contact cycles. Its only weakness was its tendency to adsorb hydrophobic contaminants, which made it difficult to keep a

given sample clean for long.

The more complex the desired shape, the more complex the procedure for fabricating the mold. A multi step fabrication often requires that different parts of the design be made using different lithographic techniques on a single given sample. This is necessary because with many of these techniques, the undissolved material is still reactive with the etchant, just more weakly than the material that had received a dose of UV light. As a result, it is impossible to perform a patterning procedure on one layer where the etchant is to come in contact with a previous, already prepared layer, if the new etchant and the old layer are reactive. In some cases it is possible to mix and match such procedures, so that etchants are only ever in contact with the desired material layer. Often the best solution is alternating a photolithographic step with a reactive ion etching step, as the plasma ions were not reactive with the photoresist, and the photoresist etchant was not reactive with the Silicon or the underlying oxide layer of which the wafers were composed [44].

An example of a typical procedure would be the fabrication of a stamp in the shape of a two-tiered cake [50]. We begin by choosing an SOI wafer with a Si layer that has the thickness we desire for the top segment. A layer of negative tone photoresist is deposited on the wafer by spin coating. Because this photoresist layer will serve only as a masking layer for etching the Silicon, the thickness of the mask layer is unimportant. We then cover the sample with a mask that has a shaded pattern of the layer we are creating – a small black dot – and perform a UV exposure of this layer, controlling the amount of

energy absorbed by controlling the exposure time. The necessary exposure time depends on the power being put out by the light source, and by the chemical formulation of the photoresist and the thickness of the photoresist layer. If a negative tone resist is under exposed, too much of the layer will remain soluble, and the developer will etch away more of our feature than we want. If it is over exposed, exposure effects will penetrate into the shaded section, and the developer will be unable to etch enough material away for our feature to come out right.

Once this first step is finished, the sample is placed in the RIE chamber and etched with Xenon Hexaflouride and Oxygen plasma. The plasma does not attack the photoresist layer or anything directly beneath it. Thus, the same pattern that was on our photomask is etched into the Silicon layer on the wafer until it reaches the bottom of that layer, leaving us with a pit that is as deep as the Si layer is thick. Alternatively, we can control the depth of this feature by controlling the length of time the sample is exposed to plasma based on known etching rates for this reaction.

Now we are left with a clean SOI wafer that already has a pattern on it. If we were to cure PDMS against this mold, we would get a simple column where the PDMS conformed to the shape of the pit. In order to add another tier to the cake, we simply add another layer of photoresist and pattern it so that a pit with a larger cross-sectional area than the first one is concentrically aligned over the first pit. In the end, we have a pit in a layer of photoresist that has a Si floor with another, smaller pit in that floor. When used as a PDMS mold, this gives us a sample with a column that has a smaller column

protruding from its top surface.

Both of the photolithographic steps explained above used negative tone photoresist, but positive tone resist could have also been used. It would only be necessary to have a negative version of the same photomask to translate this step in such a way.

Aside from the above description, there are several intermittent steps in the recipe for making these molds. These steps mainly fall into two categories: heat treatment and surface treatment. Various surface treatments such as Ozone treatment, or deposition of chemical monolayers such Hexamethyldisiloxane (HMDS) and Trichlorosilane facilitate greater or lesser interfacial tension between various layers, as needed. During the mold fabrication process, various surface treatments facilitate a better bond between the various layers of building material. At the end of the molding process itself, a layer of Trichlorosilane makes it easier to peel the PDMS stamp from the mold, which both leaves the stamp cleaner and keeps the mold from breaking, so that it may be reused. Heat treatments of varying order, duration, and temperature are also necessary when applying photoresist, and vary greatly depending on the particular recipe being used.

Ultimately, lithography is a very sophisticated set of tools, and with enough care and planning can be used to create fairly complex molds, but it has its fair share of limitations. As the above description makes evident, lithography is a difficult technique, requiring careful planning, many time and resource consuming steps, and a sufficiently clean environment. But even with these challenges met, there are also limits to the

resolution – the smallest feature that can be clearly resolved – that is achievable with these methods. The exact source of these limits differs for each of the techniques in this set of methods. Photoresists have resolution limits that depend on their viscosities, photomasks have resolution limits based on their printers' abilities, etc. – and often these issues compound one another.

CHAPTER 4

MICROCONTACT PRINTING

Microcontact printing (uCP) is a method for transferring materials – referred to as inks – from a stamp generally made from PDMS to a target substrate (**Figure 6**) [4, 35, 36, 51]. The fact that this is a micron scale method refers to both the size of the features of the inks as well as the resolution of this printing method. uCP can either be used to transfer thin films or rigid micron scale devices. For thin film transfer experiments, a gold film is a common ink candidate, while the nano and micro scale devices are generally made of semiconductor material.

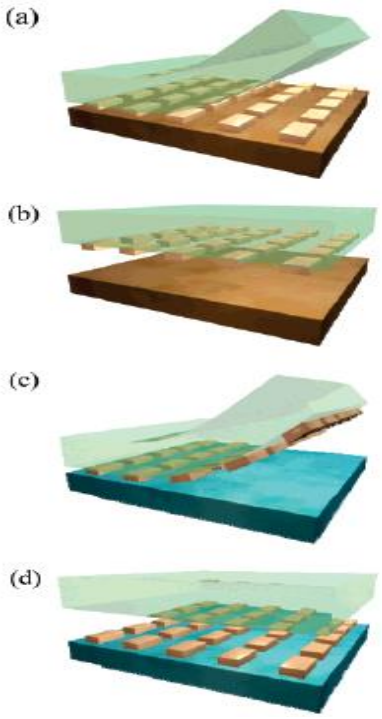

Figure 6. Schematic of generic process flow for transfer printing. First the devices are transferred from the donor substrate to the elastomeric stamp (inking) (a, b), then they are transferred from the stamp to the target substrate

The mechanics of transfer printing with a stamp made from viscoelastic material such as PDMS can be described by the characteristic energy release rate, G, associated with both the interface in question and the peeling velocity. G is a value that can be treated in a similar way to the work of adhesion in determining conditions for different printing modes. If the stamp is to pick inks up off of a substrate, then it must be that $G_{sub/ink} < G_{ink/stamp}$. If the stamp is to deposit those inks onto a target substrate, then the opposite must be true, $G_{sub/ink} > G_{ink/stamp}$.

Unlike work of adhesion, G takes into account both the bonds breaking along the failing interface as well as the viscoelastic energy being dissipated at the tip of the crack between the surfaces. Due to the relatively rigid nature of most inks and substrates – in our studies we focused on semiconductor chips as inks being printed onto Si wafer substrates – the critical energy release rate between ink and substrate, $G_{sub/ink}$ does not depend at all on the peeling velocity. Meanwhile, the stamp is viscoelastic, so the energy release rate associated with an interface made by the stamp does depend on peeling velocity. This immediately suggests that there is a velocity dependence that can be used to control whether $G_{sub/ink}$ is greater or less than $G_{ink/stamp}$.

Using a power law that is often helpful in modeling soft adhesion, we can plot the equation:

$$G_{ink/stamp} = G_0 \left[1 + \left(\frac{v}{v_0} \right) \right]^n$$

Where G_0 is the critical release rate as peel velocity approaches zero, v_0 is a reference peel velocity related to G_0, and n is a scaling parameter. **Figure 7** shows how the velocity dependence of $G_{ink/stamp}$ causes the system to switch between pick up and printing mode

where $G_{ink/stamp}$ intersects with $G_{sub/ink}$.

The energy release rate parameter, G gives us a very convenient way to view the kinetic adhesive nature of an unpatterned interface. This parameter can also be elegantly measured using a cylinder roll test, which will be discussed in detail in the following chapter. These viscoelastic effects apply in all cases with soft stamp transfer printing, although the addition of micron-scale patterning can add many significant details.

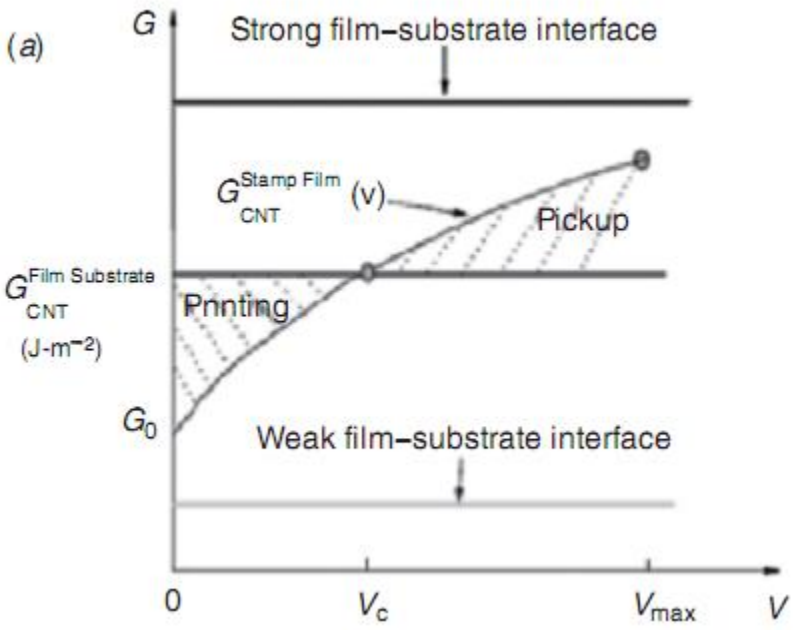

Figure 7 - Plot of energy release rate, $G_{stamp/ink}$, dependant on peeling velocity, v. When the peeling velocity is sufficiently low, the energy dissipation between the stamp and the ink is also low. If an ink/substrate combination is appropriately chosen, such that $G_{sub/ink}$, which is constant, will fall in the middle of $G_{stamp/ink}$ range, then a low $G_{stamp/ink}$ will always result in printing, as the ink/substrate adhesive forces are stronger. Once $G_{stamp/ink}$ reaches a critical level, as defined by its intersection with the constant $G_{sub/ink,}$ the adhesion between the ink and the stamp will be stronger than between the stamp and the substrate, and the system will switch to pickup mode. These functions depend as much on the shape of the $G_{stamp/ink}$ as they do on the value of $G_{sub/ink}$. This is illustrated by the three different levels of $G_{sub/ink}$ shown on the graph. If the ink/substrate interface is too weak, the system will always be in pickup mode, and if it is too strong, the system will always in printing mode.

Transfer printing of gold films is a somewhat more chemically sophisticated process than the dry adhesion necessary to print semiconductor inks, but many of the

biomimetic principles that serve as inspiration for this work are applicable to the design of stamps meant to transfer macroscopic gold films. Gold is arranged on the surface of the PDMS stamp via thiol chemistry, which forms self-assembled monolayers (SAMs) on a surface because of the structure of the thiols (**Figure 8**) [52]. Thiols are molecules consisting of a hydrocarbon chain that has at one end a "head group" capable of bonding to PDMS, and at the other end another functional group. Thiol-metal bonds have a bond energy on the order of 100 kJ/mol, so the bond between a thiol and a Gold atom tends to be very stable [53]. Van der Waals attractions between the thiols also facilitate tight packing, creating a smooth monolayer .

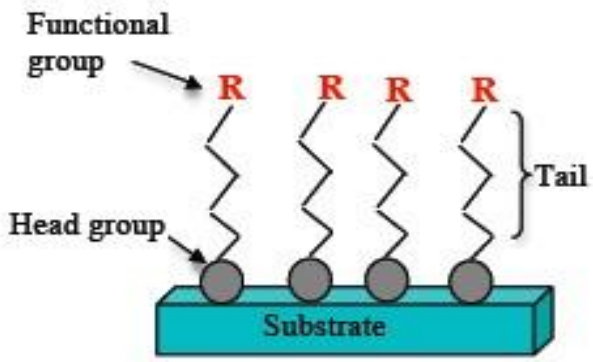

Figure 8 - Thiol self-assembled monolayer (SAM) schematic showing the head group attached to the PDMS substrate and the functional group which allows the chain to bond at the other end with a Gold atom. http://en.wikipedia.org/wiki/Self-assembled_monolayer

While thiol chemistry obviates the need for dry adhesion in the transferring of such metal films, many of the more mechanical features and phenomena that arise from the study of biomimetics are applicable to this technology. By considering how interfacial cracks propagate, for example, we can use a PDMS stamp in such a way as to give it a particular set of transferring capabilities. The simplest effect is derived from the motion breaking apart

the interface. A PDMS stamp which is inked with a Gold SAM, and then brought into contact with a target substrate with a comparable affinity for Gold, can be peeled quickly or slowly. While the exact regimes of the peel velocities depend on everything from the geometry of the system to the particular chemistry and energy associated with those interfaces, the binary effect is clear: Peeling slowly allows the thiol tails to stretch and break, printing the Gold on the target substrate, while peeling quickly keeps the SAM from relaxing in this way, and in so doing keeps the Gold on the stamp [52].

Microstructural patterning can also be used to make use of this relaxation effect. If the stamp surface is patterned with small periodic pits or grooves whose depth is great enough that it is easy for them to experience roof collapse – as described in the section on adhesion – when placed under a small amount of pressure, but not so great that roof collapse is favorable without this added pressure, the effect of relaxation time competing against peel rate is compounded. If the inked stamp is peeled slowly, the roofs retract upward, holding some of the Gold layer with them. If, on the other hand, the stamp is peeled quickly, the crack between the Gold layer and the stamp can propagate before the roofs decollapse, thus facilitating transfer to the target substrate [3, 17]. A schematic representation of the phenomenon roof collapse is

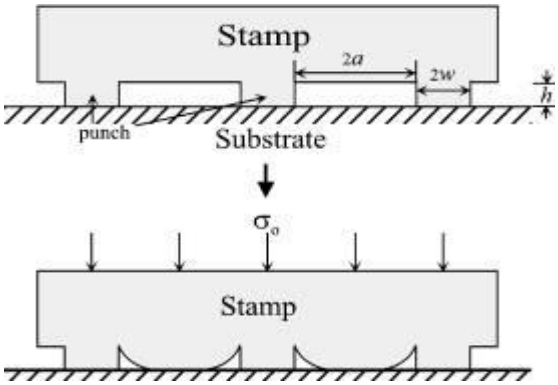

Figure 9 - Roof Collapse of a structured PDMS stamp. The top panel is the molded shape of the stamp. The bottom panel shows collapse which occurs under favorable conditions, namely that the dispersive adhesion between the surfaces can overcome the structural integrity of the elastomer material [3].

shown in **Figure 9** [3].

Huang et al have developed a micromechanics model for roof collapse without the external load to establish a criterion for roof collapse in soft lithography [3]. This micromechanical model is based on the premise that roof collapse will occur when the collapsed state is a lower state of energy than the uncollapsed state. This view divides the possibility of collapse into three situations unstable collapse, in which collapse will only occur when an external load is applied to the backing layer and if that external load is removed the roof will return to its original shape, stable collapse, in which collapse occurs naturally without any external load because of the dispersive attraction between the PDMS and the substrate, and metastable collapse, in which collapse will also only occur after some external load, but the stamp will remain in the collapsed state after the load has been removed.

Which behavior a stamp will demonstrate depends on the specific work of adhesion between the PDMS and the substrate, γ, the elastic modulus of the PDMS (E), in this case taken as the plain-strain elastic modulus, $E' = E/(1 - \nu^2)$) 4/3E, where the poissons ratio is $\nu^2 = 0.5$, and the physical dimensions of the punches, a and w are feature widths as labeled in **Figure 9**. For instance, if a >> w, the of equation that determines the stability of collapse is:

$$\frac{4a\dot{\gamma}}{E'h^2}\frac{8}{\pi^2}\left(1+\frac{w}{a}\right)^2 \ln\left[\sec\left(\frac{\pi}{2}\frac{1}{1+\frac{w}{a}}\right)\right]$$

If the value of this equation is >0.83 but < 1.4, then collapse is metastable. If that figure comes out to be less than 0.83, then collapse is unstable, whereas if it is greater than 1.40, collapse is automatically stable [3].

In our research, we designed stamps whose function depended on their being somewhere around the nexus of metastable and unstable collapse. A stamp such as this can exhibit passively tunable adhesion because there is a stronger adhesion between the stamp and the potential ink during the collapsed state, when there is full contact between the roof and the ink, than during the uncollapsed state, when only the periodic punches are contacting. So long as the collapse is just favorable enough that once the load is applied, the stamp retains the collapsed state while it is being retracted and until after the interface between the ink and the donor substrate has been broken, we will be able to take advantage of the collapse. Ideally, after this inking event is complete, the stamp roof will decollapse as result of the stress and pulling force of the retraction. The inked stamp may then bring the ink over to a target substrate and gently place it down, taking care not to load the stamp enough to cause collapse again. Since the deposition step will happen while the roof is not collapsed, the adhesion between the stamp and the ink will be weaker, thus facilitating deposition. This function is referred to as passively tunable adhesion because the tunability is not controlled by any additional mechanism. It is controlled by the load placed on the backing layer, and more importantly, by the speed of the retraction. A fast retraction facilitates inking by completing the inking event before decollapse occurs. For this reason, this method is also referred to as kinetically controlled transfer printing.

Micro-patterning of large-area stamps has also been shown to decrease imperfections in thin film transfer printing [54]. Flexography, which is essentially a form of transfer printing that uses a flexible, large-area stamp with a smooth surface, has demonstrated an inability to transfer thin metal films without imperfections such as breaks and point distortions. By micro-patterning the surface of the flexographic stamp, such imperfections can be minimized in thin films as large as one square foot.

Semiconductor ink chiplets, which are the main focus of this thesis, adhere to PDMS surfaces by dispersive adhesion, and so do not require SAM chemistry to be transferred via uCP [55]. The practical usefulness of these materials is obvious – because of their mechanical and electrical properties, they serve as the basis for a variety of microelectromechanical systems (MEMS). Semiconductor inks in the shape of micro and nano sized squares can be used to build many different types of sensors, actuators, and physical structures that can be used to create devices such as molds, patterned surfaces, microfluidic devices, micromechanical devices, etc.

These inks are produced by an etching procedure composed of several steps such as the ones described earlier. In our research the semiconductor inks were Silicon, and batches of these inks were fabricated in the following way: An SOI wafer with a layer of Si [100] on the top is patterned by coating it with a layer of photoresist which is then photolithographically patterned with a grid. The sample is then etched by RIE (Sulfur Hexaflouride plasma), to transfer that pattern into the Si layer, which is now divided into a grid of square platelets, 100 um to a side, with a 300 um separation distance between

each chip. Next, the photoresist is cleaned away, and some of the buried oxide layer on which the Si is resting is etched away with Hydroflouric acid. This etching gets rid of the oxide in the separation region between the plates, and undercuts some of the oxide directly underneath the chips. The HF solution is not permitted to completely finish etching away the oxide layer, as this would leave the chips free floating, and lose them. To prevent this, a second layer of photoresist is applied and patterned into small, rectangular, mechanical anchors, which overlap with the inter-platelet separation region and the corners of the platelets themselves, thus tethering the Si chips to the underlying substrate. Once these anchors are in place, the remaining buried oxide layer can be safely etched away, leaving our patterned chips supported only by brittle photoresist anchors which are easy to break.

The challenge in the printing of semiconductor inks is the low threshold for distortion. In order to construct complicated devices with the necessary level of precision, the stamp must be able to cleanly pick up the ink, hold it stably as it is being transported to the target, and place it gently on the target without having the ink jump around or reorient itself in an uncontrolled way. To maximize the resolution of this printing process, the printer machine must also be capable of articulating very fine motion. The latter is achievable with high-end motorized stages, capable of articulating minute translational and rotational motions. The former depends on the microstructural design of the stamp, which will be the focus of the section on microstructures.

In short, by focusing more closely on the micron-scale adhesive events occurring

at the interfaces of the transfer printing system, we can improve on the reliability of the transfers, as well as decrease the occurrence of random imperfections in transferred thin films, and increase the precision and fidelity of our MEMS constructing technology.

CHAPTER 5

EXPERIMENTAL SETUP

Having fabricated our stamps and our inks, we can load them into our transfer printer to begin testing. In order to effectively report both quantitative and qualitative results, we need a system that is capable of precise, reproducible fine motion, provides tangible quantitative data regarding attractive forces doing work at the relevant interfaces, and allows us to see what is actually occurring at those interfaces. The setup that was used to perform these experiments is shown in **Figure 10** and described in our recent study [7].

In this setup, the inks and the target substrate were mounted on a motorized stage capable of x and y translational motion. This stage was capable of motions as small as a tenth of a micron, and the velocity could also be controlled to within 0.1 microns per second. For the acquisition of quantitative results, the target substrate could be mounted on a ten gram load cell (part names/specs), which we used to resolve forces in the millinewton and sub millinewton range. Pressing down on the load cell would register a positive compressive force, and then pull-off would be detected as a negative tensile force as the load cell arm is pulled up with the apparatus until interfacial failure occurs. The difference between the maximum tensile force and the zero level is considered the total tensile force exerted by the stamp as it is being pulled off, and this number was treated as the ultimate result of these experiments. In our study, this value was deduced from plots of load cell data, as demonstrated in **Figure 11** [7].

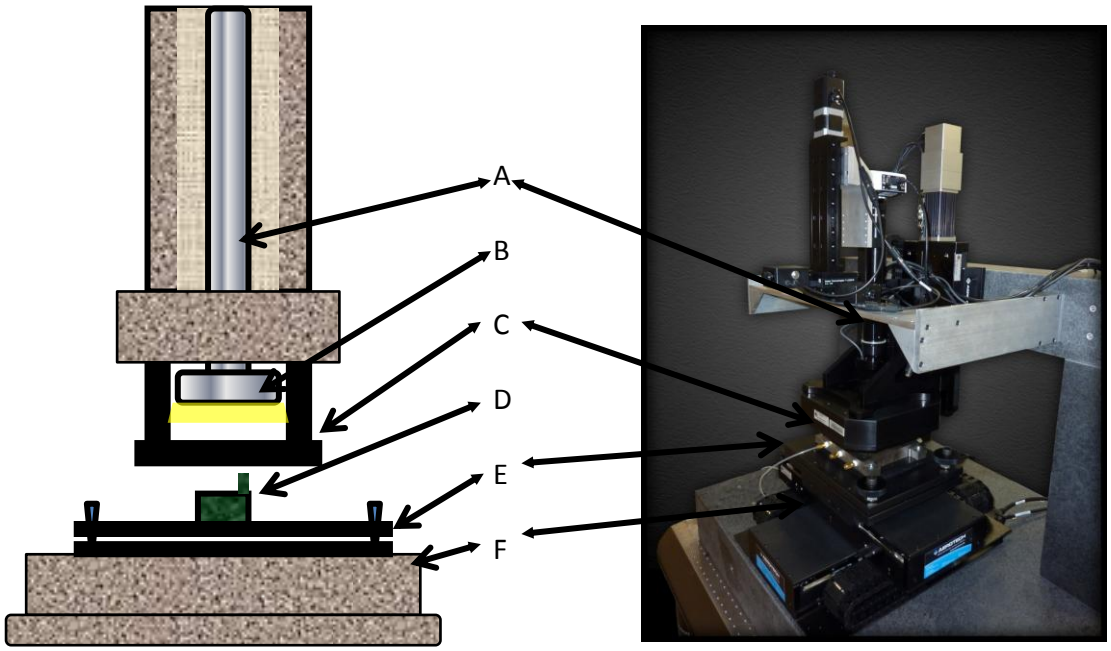

Figure 10. Schematic of transfer printer used for our experiments. The setup was designed to facilitate a direct view of the PDMS/substrate interface concurrently with load cell data acquisition. The column containing the optics (A) and a circular LED light source attached to the end of that column (B) were mounted above the sample-holder stage (C). The sample-holder stage was capable of z-axis and rotational motion, and had a transparent area in the middle where a clear glass slide holding a PDMS sample could be mounted and held by vacuum. Z-axis motion of the sample-holder stage was used to load and unload the stamp by pressing down and pulling off of the 10 gram load cell directly underneath (D). A small piece of an Si [100] wafer was mounted on the tip of the load cell. Because all layers between the Si and the optics were transparent, it was possible to watch and digitally capture action at the Si/PDMS interface. The load cell was mounted on a tip/tilt stage (E) to ensure normal loading, and on top of a translational stage capable of x-y motion which facilitated shearing motion experiments. The optics and light source moved together and were capable of x-y-z motion.

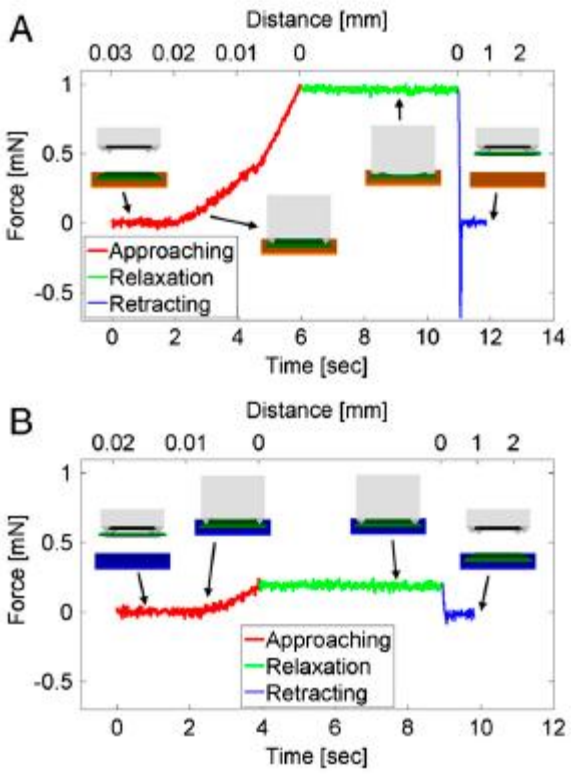

Figure 11. Load cell data plots of adhesive force associated with normal loading of pyramid stamps in an inking cycle (A) and a printing cycle (B). (A) In the inking cycle, during the approach, two slopes are clearly visible. The first slope is associated with the deformation of the raised features, and the second slope appears when roof collapse occurs and the bulk of the stamp begins deforming. The stamp is then allowed to relax for 5 seconds, during which time the load cell registers a constant load. After this dwell time, the stamp is rapidly retracted from the substrate. The load cell registers a negative pulling force and then returns to its zero level. The difference between the negative peak and the zero level is taken as the adhesive strength of the stamp in this inking mode. (B) shows a printing cycle, in which roof collapse is not allowed to occur. The reduced contact area at the moment of retraction results in negligible adhesion,which is clear from the plot because the load cell registers very little or no negative pulling force when the stamp is retracted, just before the load cell returns to its zero level [7].

However, other features of the force vs. time plot were also taken into consideration for the specific information they provided about each trial, such as the preload – the force with which the stamp is initially pressed down – and the lengths of time required for the plot to reach equilibrium in the absence of motion, which depended on the relaxation behavior of both the stamp and the load cell itself.

The stamp was mounted above the stage on a holder that held a glass slide in place by pulling vacuum. This holder had a hole in the middle which allowed us to place motorized optics above the system and look directly through the transparent glass slide, through the transparent PDMS stamp, and focus our optics directly on the ink or target substrate. This setup provided us with an excellent view of the interface between the stamp and whatever opaque surface it was contacting with. We were able to capture stills and movies of a high enough quality that they could be discussed qualitatively and analyzed quantitatively with imaging software for effects such as delamination rate and percent contact area during partial contact (**Figure 12**). This arm is capable of vertical motion with the same resolution as the translational stage, and is also capable of rotational motion with a precision of down to a tenth of a degree.

The optics are mounted above this set up looking down through the stamp holder onto the stage at the bottom. The optics are also motorized with the same motion resolution as the stages, and capable of both horizontal and vertical translational motion. All of the motion is controlled by software designed specifically for use in our lab, and gave the user the ability to control printer motion in real time, as well as to set a series of

pre-programmed motions to follow. However, before we implemented this system, we used a few other simpler methods for testing the adhesive characteristics of macroscopic stamps with microstructural patterning on their surfaces.

A

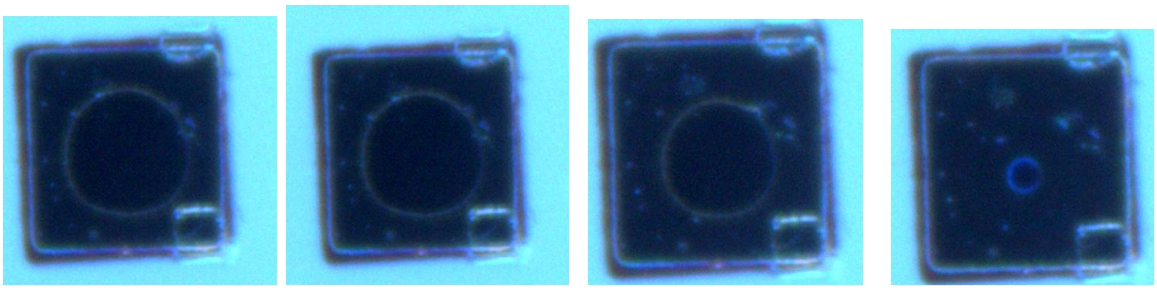

B

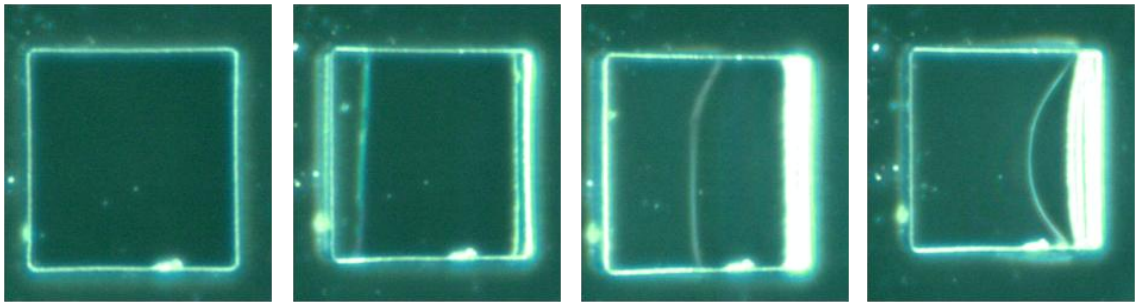

Figure 12. Time elapsed stills captured on Transfer Printer in Mechanical Engineering Laboratory, UIUC. The optical setup allowed users to view detailed events in real time. (A) shows a slow delamination which took about 10 minutes - the dark circle is the contact area between a structured PDMS stamp and a semiconductor chip, which slowly grows smaller as the PDMS delaminates from the chip. (B) shows the changing contact area between a flat PDMS post and a Si substrate as the post is being dragged to the right across the Si surface.

When testing stamps that did not need micron-level resolved motion, there were a couple of simple testing methods at our disposal. These methods were useful when testing stamps for their large-area transfer capability, which is to say mostly for thin film transfer. Some of the stamps we produced were patterned with long, microscopically narrow grating structure. These were fabricated to test the effect of directionality in peeling force – researching the functional difference in peeling such a stamp from a surface such that the delamination occurs parallel vs. perpendicular to the orientation of the grating structure. Some stamps were fabricated with groupings of pits to test the effect of delamination velocity competing against roof collapse and relaxation, the independent parameters being the dimensions and packing arrangements of these pits. With stamps like these, we were only interested in the force and delamination rate associated with peeling patterned areas between 1 and 10 square inches.

The simplest test devised for this purpose we refer to as the hanging weight test. A thin, patterned PDMS stamp is brought into contact with a clean glass substrate, and suspended in a horizontal orientation, with the support holding the glass plate, and the stamp stuck to the downward facing surface. A weight would then be attached to the edge of the stamp with a binder clip. The primary goal of such an experiment would be to find critical weight required to cause delamination.

Another simple and elegant test that we also used in this study is the cylinder roll test [51]. In this test, a steel cylinder is rolled down a microstructured surface on an inclined plane .The adhesive energy between the cylinder and the sample surface

competes against the gravitational potential pulling the cylinder down the incline.

The difference between the gravitational potential lost:

$E_G = mgh$

where m is the mass of the cylinder, g is the acceleration due to gravity, and h is the change in the vertical distance,

and the total kinetic energy:

$E_K = (v^2)m/2 + (\acute{\omega}^2)I/2$

where v is the velocity of the cylinder and ώ is the speed of the cylinder rotation and I is the cylinder's moment of inertia,

is the energy that is absorbed by the substrate's adhesive action (E_G - E_K) [51].

When these forces reach an equilibrium, the cylinder reaches a terminal velocity, which means that the terminal velocity is a direct function of the adhesive nature of the substrate on the incline [51]. The substrate's adhesion simply acts as a force of drag. This energy is referred to as the energy release rate, G, of the system, and can be plotted against the velocity, v of the cylinder. Technically, this energy release rate is also the difference between the energy released at the trailing edge of the rolling cylinder, where the cylinder surface is continuously separating from the inclined substrate, and the energy evolved at the leading edge of the rolling cylinder, however the energy evolved at the advancing contact area is typically small [56]. When adhesion is strong, a high velocity implies a high energy release rate.

Both of these simpler methods suffer from a lack of robustness – conclusions from their data strongly assume ideal experimental behavior – and both methods are somewhat esoteric, since extrapolating these data to any geometries aside from those of the experimental setups is very complicated. The use of an automated transfer printer as described above greatly simplifies the acquisition and analysis of adhesion data, since it answers the question of "how much adhesive force is being exerted" much more directly, and it allows us to perform experiments on whatever size sample we like, rather than having to extrapolate on a per area basis.

The transfer printer, on the other hand, falls prey to a variety of effects that obscure the desired data. Relaxation times in both the PDMS stamp and the load cell mechanism itself, as well as static charge build up caused by repeated contact cycles can register on the adhesion plot acquired by the load cell. Messy load cell plots can be caused by jogging – jerking motions that occur due to imperfect mechanical behavior in the motors of the transfer printer stages. Tilt misalignment creates disparity between what is being observed and how it is interpreted because in modeling it is assumed that the PDMS sample surface is parallel to the ink or substrate surface. Particulate contamination is also more of concern when working on the micron scale. If a fiber on the surface of a 100um x 100um stamp is one micron wide and one centimeter long, then it constitutes a 1% coverage of the stamp surface. In order for a 10cm x 10cm stamp to have 1% of its surface covered by such contamination, it would have to have around 10,000 such fibers.

In our setup, each of these issues were addressed individually to optimize the

quality of the results. A grounding device was constructed out of a metal wire and a metal disc, and was used to discharge the stamp as needed. The bottom stage was constructed with a tip-tilt system that allowed us to tilt the stage to make sure the substrate it was carrying was parallel to the stamp. The whole system was kept in a modular clean room environment, and exfoliating cleanings using scotch tape were applied liberally to all substrates and samples. The equipment was set up on a floating table to minimize the effects of vibrations on load cell readings. Unwanted effects due to jogging and relaxation effects were dealt with in the software controlling the printer, by making certain that the motion protocols had pauses at appropriate moments allowing for relaxation and periods of slower motion as the samples approached contact to avoid unnecessarily hard impact that could affect the behavior of the stamp during the following cycle, or even damage the load cell.

The software controlling the printer motion also allowed us to test motion related parameters that affect strength of adhesion. As discussed earlier, the rate at which an adhesive interface is broken has a strong effect on the energy required to separate those surfaces. Many of our designs were created with the purpose of exploiting this phenomenon, and so many of our experimental methodologies involved testing the dependence of adhesion on retraction velocity – the rate at which the printer machine pulled the adhesive sample off of the target substrate. We also explored the effects of shear motion on adhesion, which has been shown to dramatically reduce adhesive strength. The motion control software enabled us to perform a wide variety of experiments accounting for different sorts of possible motions which our stamps were

designed to exploit.

CHAPTER 6

MICROSTRUCTURAL DESIGN & ANALYSIS

In this section I will discuss the specific types of microstructural features that can affect the adhesive character of a patterned surface, focusing on features fabricated and tested in our studies. For the most part, these features can be divided into two categories: Features that increase adhesion and features that decrease adhesion. Conceptually speaking, features that increase adhesion are ones that maximize the amount of interfacial contact and resist the occurrence of separation, while features that decrease adhesion are ones that minimize contact and facilitate quicker, more energetically favorable delamination.

The first design parameter that we considered when making any sort of structure is the material itself. In this case, the most important quality of the material is its elastic Young's modulus. As discussed earlier [5], improved conformal contact is one of the simplest ways to dramatically increase adhesive strength. It is on this basis that biological systems enhance their ability to adhere to substrates, from insects, spiders, and geckos walking upside down or on vertical surfaces, to plant seeds that rely on their ability to stick to other surfaces to spread their genetic material across their habitats. Natural surfaces tend to be very rough – such as rock faces and tree bark – so contact splitting facilitates better conformal contact because it allows more contact elements to make contact with parts of the surface that would otherwise be obscured by roughness. In our experiments, roughness was much finer, so to facilitate conformal contact we used a formulation of PDMS with a low elastic modulus. This allowed the stamp surface to warp

and bend around any surface roughness to touch down at spots that it would not be able to reach if the surface were rigid. We sometimes used different formulations of PDMS in order to test elastic modulus as a controlled parameter. PDMS that was mixed with a ratio of ten parts polymer to one part cross-linking catalyst has an elastic modulus of 2.8 MPa, and this was the formulation used in all cases discussed in this thesis, except when otherwise specified [3]. When a different elastic modulus was desired, a formulation of 5:1 PDMS to catalyst was made, which would be twice as stiff [7].

One of the geometric features causing increased adhesion that we tested are ones that redistribute stress away from where crack initiation is most favorable, which is to say, the edge of the interface [57]. If a normal force is applied across an interface to break that interface, stress concentration at the perimeter of the interface will cause a crack to initiate there. That crack will then propagate with relative ease from the perimeter inward toward the center of the interface until contact is completely broken. If, however, this normal force pulling the surfaces apart is not distributed uniformly along the entire interface, we can see a different effect emerge (**Figure 13**).

To demonstrate this concept on a macroscopic level, we constructed what we call stem-and-pad stamps out of PDMS. The mold was made-to-order out of high density plastic and surface coated with a layer of tricholorosilane to facilitate easier removal of the molded PDMS sample from the mold itself. Each stamp had two sections: The pad, which is a wide, thin piece with a flat surface, and a stem, which was long and narrow. The pad was the part that stuck to the target substrate with its flat bottom surface via dry

adhesion, while the stem served essentially as a handle protruding from the top of the pad. The macroscopic samples were molded to be about four inches tall, usually with circular shapes with the pad having a radius of about two inches, and the stem having a radius of about half an inch.

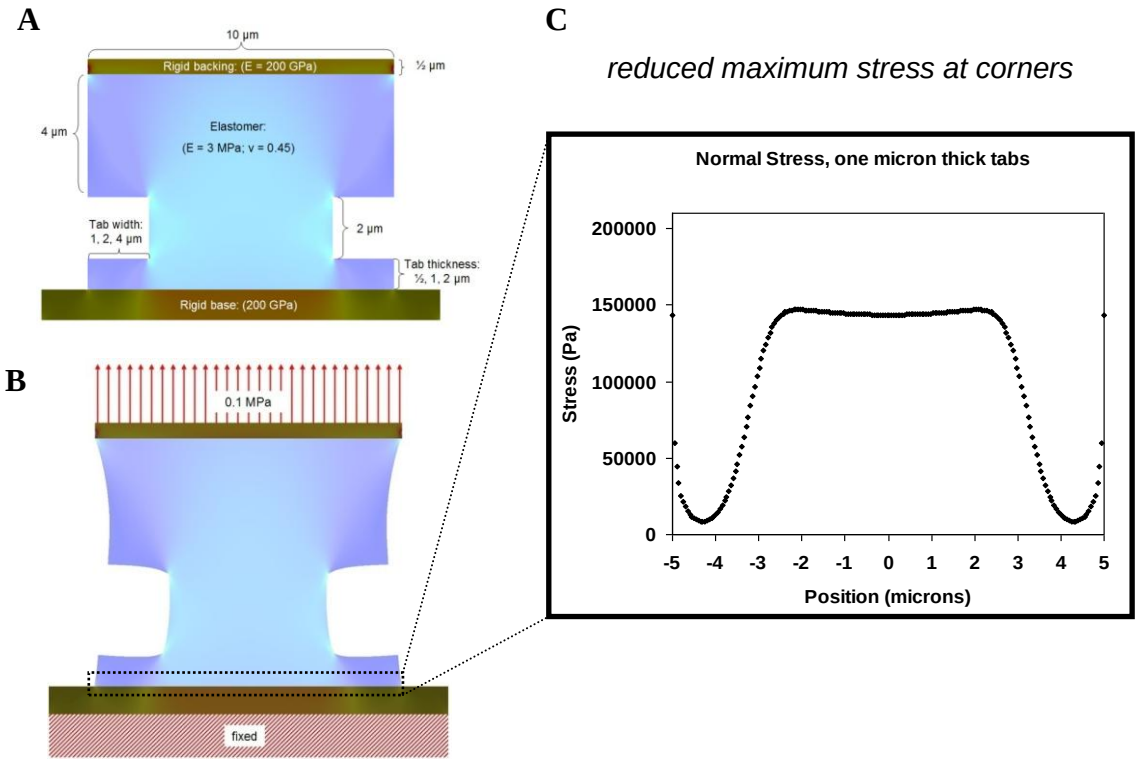

Figure 13. Finite element simulation of stem-and-pad PDMS stamp form factor. (A) Stamp at rest on surface. (B) Stamp with normal, upward pulling load. Light blue indicates areas of higher stress. The loaded stamp (B) and the corresponding plot of stress vs. position (C) show stress concentrating directly underneath the stem portion, and away from the perimeter of the pad. A threshold of stress must be reached at the perimeter of the adhering interface in order to initiate a crack there. Because stress is distributed away from the interface perimeter, a much greater pulling load is required to accumulate the stress required to break this interface. In practice, the PDMS stem undergoes catastrophic tensile failure before the interface is broken [57].

The pad's bottom surface would then be stuck onto a surface – most any clean, flat surface would do, such as a glass plate or the resin surface of the average laboratory bench – and the strength of this dry adhesive interface would be tested by pulling on the stem. Because the stem's radius is so much smaller than the pad's, the stress which would otherwise be concentrated around the perimeter of the interface, is actually concentrated around the perimeter of the circular area directly beneath the stem. This is where the crack must initiate, so rather than propagating from the interface perimeter inward, it must propagate from the center outward. This geometry is highly unfavorable for crack propagation. Portions of the elastic pad surface that have been pulled away from the substrate are being pulled back down by adjacent PDMS material from all directions, except for the direction pointing toward the center. Without the stem-and-pad design, the opposite is true: portions of the pad surface that have already lifted off are only being pulled back down by neighboring material still stuck to the substrate in the direction of the center, while material in all other directions has already been lifted off as well.

In fact, this force keeping the interface intact is so strong that even if a normal force great enough to initiate a crack at the center of our stem-and-pad sample interface, that force may not be great enough for the crack to propagate. It would simply advance some distance out from the center and stop indefinitely until the normal force was turned off, restoring the entire interface, or the normal force was increased, causing the crack front to advance proportionally further outward from the interfacial center. Conversely, without the stem-and-pad design, once a normal force was sufficient to create even a very small separation at the interfacial perimeter, this crack would easily and usually

instantaneously propagate through the entire interface, and contact would be immediately broken. In this way we demonstrated that the stem-and-pad design increased the adhesive strength of such a stamp by many orders of magnitude from a simpler geometry without engineering any sort of adhesive chemistry. In fact, this adhesion was so strong that often the stamp itself would break – the stem would be torn off of the pad – before the interface broke.

It is reasonable to speculate that this geometry had other emergent effects that contributed to this high adhesive strength, although they are difficult to test and therefore outside the scope of this work. For one, it is possible that the void created at the center of the interface as the surface began to be pulled apart exerted a significant force caused by vacuum effects and pulled the surfaced back together. It is difficult to determine the strength of this effect due to phenomena which could negate the creation of a vacuum, such as air flowing into the void at the interfacial center either through tiny rivulets along the interface itself or via diffusion through the PDMS.

What we demonstrated with these experiments macroscopically can be observed microscopically as well. In biomimetics, this can be seen in the spatula shape of the contact elements of some animals, most notably geckos. By having hairs with setal pads that are much wider than the stems connecting those contact elements to the gecko, each singular contact element exhibits this stress redistribution effect. Each one of the millions of setae is therefore orders of magnitude stronger than it would be if it were a fibril with a simpler geometric form factor. In microstructure design, this effect has also been shown.

Research in other groups has shown that molds made with some undercutting – which causes the bottom surface of the molded PDMS to be wider than the area connecting each microstructure to the bulk PDMS – also facilitates dramatically increased adhesive strength for a micropatterned surface fabricated using such a mold. This effect is observed in a variety of surface geometries, which is to say whether the bottom surface is circular or rectangular or even if the pad is only wider than the stem along one dimension and not the other. This makes the stem-and-pad concept a fairly versatile feature, as it can be incorporated into a microstructure in a variety of ways.

As a consequence of the stem-and-pad experiments, some questions arose about the presence of vacuum effects**.** Although a small void is created when the center of the stem-and-pad stamp surface was pulled up, it was difficult to conclude how much if any vacuum force this void caused. Air could diffuse in undetectable channels through the contacted interface into the void, or it could even diffuse into the bulk PDMS, relieving vacuum pressure from the interface. In order to test for the possible presence of vacuum effects, we fabricated several stamps with walls or "lips" (**Figure 14**). When brought into contact with a smooth substrate, the stamp would make a small rectangular chamber, and when the roof is forced to collapse the air is squeezed out of this chamber. If vacuum

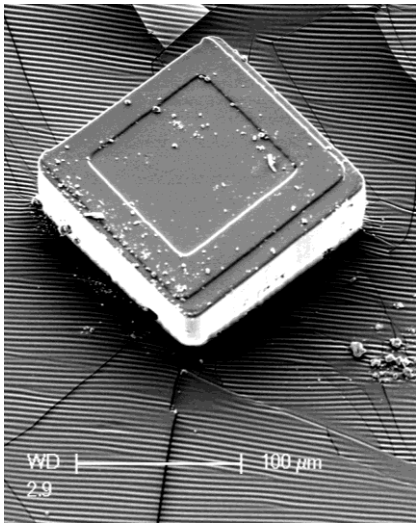

Figure 14. SEM image of PDMS stamp with a square lip. Stamps of varying wall thickness were fabricated to verify the presence of vacuum suction effects on the overall adhesive strength of such stamps. Significant decrease in decollapse rate indicated that suction was indeed holding the stamp in the collapsed state.

effects are absent or negligible, then the roof should automatically decollapse, whereas if there is a vacuum affecting the system, the suction it creates will hold the chamber in the squeezed, collapsed state.

After testing stamps with varying wall thicknesses, we found that there were indeed some vacuum effects. As per figure 12(A), we observed that in a situation where the stamp's form factor facilitated suction, delamination occurred at a far slower rate. To confirm these results, we then fabricated a similar set of stamps with square lips, but this time we added air inlets (**Figure 15**). Flow rate of air into a chamber can be approximated as:

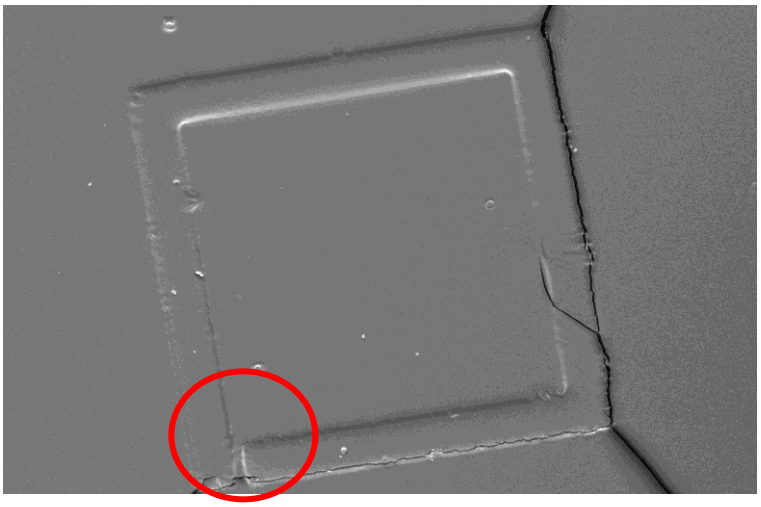

Figure 15. SEM image of PDMS square lip stamp with 1 micron wide air inlet. By adding an air inlet to the stamp designs that had shown slow decollapse due to suction, the rate of decollapse went back to being nearly instantaneous.

$$V/A=\sqrt{(2\Delta p/\rho)},$$

where V is the volume flow per unit time, A is the cross-section of the channel, Δp is the pressure difference between the inside and the outside and ρ is the density of the fluid or gas flowing through the channel. Thus, a 10^4 μm^3 chamber with a 1 µm wide gap would fill in about 20 microseconds. As we expected, all effects attributable to vacuum suction disappeared within this negligible timespan. This result was encouraging as added yet another element to the list of features that could be incorporated into a design to

manipulate its potential adhesive strength.

However, we wished to see if we could take the practical usefulness of such a feature a step further. By tailoring the exact dimensions of the air inlets, we hoped to make the added adhesion of such a feature tunable. If we could design an air inlet channel with precise dimensions that controlled the rate at which air flowed back into the chamber, then we would be able to control the strength of the adhesive interface simply by controlling the rate at which we retract the stamp. If the stamp is retracted quickly before the air inlet allows the chamber to depressurize, the adhesion would have the added strength due to vacuum. On the other hand, if the stamp is retracted slowly, the air inlet will depressurize the vacuum, and the force of the suction will not be exerted on the interface when that interface is ultimately broken. At first, we attempted to control this effect simply by reducing the size of the air inlet, but we found that our fabrication techniques had a resolution that limited the width of the air inlet to about 1 micron. A 1 micron wide channel in the square lip was enough to entirely eliminate the beneficial effects of suction within a fraction of

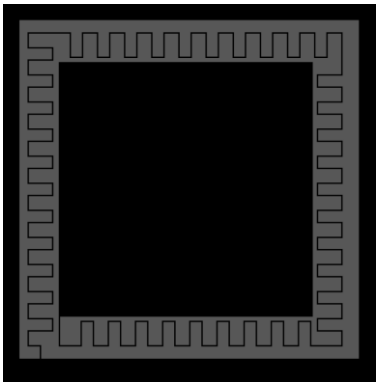

Figure 16. Schematic of photomask used to fabricate a vacuum stamp with a specialized air inlet. The channel that would depressurize the vacuum in the central chamber was 1 micron wide, and its length was increased to about 1 mm by giving it a serpentine path through the bulk of the PDMS wall surrounding the inner chamber. Fabrication of such a channel turned out to be too challenging for the techniques used in our research.

a second – much too quickly for us to take advantage of it. According to fluid dynamics, the rate of flow of a gas or fluid through a channel is inversely dependent on the channel's length. With this in mind, we designed several stamps with square lips that had the air inlet channel snaking around the perimeter of the inner chamber through the wall itself (**Figure 16**). Unfortunately, this did not properly circumvent our fabrication resolution limitations. Even with the increased length, the channel width necessary was not achievable. When we attempted to fabricate these stamps it was clear that the channels in the mold were too irregular and too fragile, and it was impossible to mold a PDMS stamp against them using the techniques available to us.

Crack arrest is another phenomenon which can be incorporated into microcontact printing to increase the maximum adhesive load, although in this case, it is a feature that is mainly applicable to larger transfers such as thin films. The concept of crack arrest is a consequence of the fact that more energy is required to initiate a crack than it does to propagate one. The equation that describes the maximum stress at the tip of a crack is

$$\sigma_{max} = \sigma \left(1 + 2\frac{a}{b}\right) = \sigma \left(1 + 2\sqrt{\frac{a}{\rho}}\right)$$

where σ_{max} is the maximum stress, $\sigma_{[0]}$ is the applied nominal stress, a is the crack length, and rho is the radius of the crack tip. It is clear from the equation that the controlling factor is the lever action of the separating crack, which depends on the ration of the crack length to the crack tip radius. If we extrapolate this logic to a flat surface, then the crack tip radius is very large, and the stress in turn is very small. On the other

hand, if there is a sharp notch and the crack tip radius is very small, and especially if the crack length is long, then the leverage of the nominal tensile stress will translate to a much greater maximum stress.

As a consequence, more energy is generally required to initiate a crack than to propagate it, and thus an interface can be strengthened against total delamination by adding features to that interface that arrest a crack as it is propagating across that interface, requiring that crack to be reinitiated.

Crack arresting features are small, periodic voids within a bulk or interface. Once a crack reaches the void that separates one microsection of the interface and the next, the crack must be reinitiated. To be precise, the amount of energy required to propagate a crack is proportional to the distance the crack is being propagated, therefore it is more accurate to say that the energy required to propagate a crack CAN be equal to that which is required to initiate a crack, once the propagated length is great enough. Apropos, enhancing the function of an interface by infusing it with periodic voids depends on the exact dimensions of those voids relative to the interface itself. A counterexample would be a notebook page with a line of perforation that facilitates cleanly tearing the page from the notebook. The line is made of periodic incisions which are relatively long compared to the material connecting the page to the binding of the notebook. As such, breaking the entire page away from the notebook binding along this line is much easier than it would be without the perforation. In this example, the crack arresting effect is overshadowed by the minimized contact between the page and the binding. In order to increase the energy

required to completely separate an interface, the voids should be small relative to the areas of contact, as the length of each void contributes nothing to the strengthening of the interface; only the presence and packing density of voids do.

To test this phenomenon, we fabricated simple grating patterns with varying inter-void distances. The sample surface consisted of a pattern of long periodic lines separated by long, narrow channels that acted as crack arresting voids. The adhesive strength of this surface was meant to be tested along a single peeling direction, which is to say, the amount of energy required to peel this surface away from a clean, flat substrate, where the peeling direction was perpendicular to the lines and channels of the pattern. The independent parameter was the packing density of the voids. We speculated that the more voids could be packed into the interface along the designated peeling, the more energy would be required to separte the interface, so long as the amount of area that was not in contact at the interface did not exceed some threshold beyond which the interface would only weaken. The more instances in which a crack has to be reinitiated rather than simply propagated, the more overall energy would be required to separate the surfaces. The stamp was fabricated using the standard photolithographic techniques mentioned earlier. Because the pattern is a simple one, the specific photolithographic recipe is not important, as almost any of the lithographic techniques described could be used to pattern such a surface.

Just as there are features that can increase adhesive strength, there are those that decrease it. For instance, it is possible to construct a feature that is essentially the opposite of the aforementioned stem-and-pad form factor. By having the contacting

surface be smaller than the size of the stem, the amount of stress required to initiate delamination is actually reduced. This has been demonstrated by research that compares the effects of a contact surface that flares out versus one that tapers in. When the stem-and-pad shape is reversed, the force required to separate the interface becomes much smaller. Geometrically speaking, this phenomenon occurs when the sample surface is convex from the point of view of the flat substrate. Taken to its logical extreme, this would be the same as a rounded surface contacting with the target substrate. The more horizontal the taper of the walls leading up to the contacting surface, the more it is as if the crack has already been initiated. If the contacting surface were hemispherical, that would be exactly the case, and only the energy required to propagate the crack would be necessary, since there would be less of a boundary at which the crack must be initiated.

Incorporating this feature into a design is very simple. Any sort of inward taper around the contact surface would drive the necessary pull-off force down, and rounding that surface would have a similar effect. In our most successful design, we fabricated a stamp with groupings of tetrahedral pyramidal tips on its surface (**figure 17**). The walls of the pyramid tapered in toward the tip of each pyramid, and tips themselves were fabricated to be so small that they were essentially rounded surfaces.

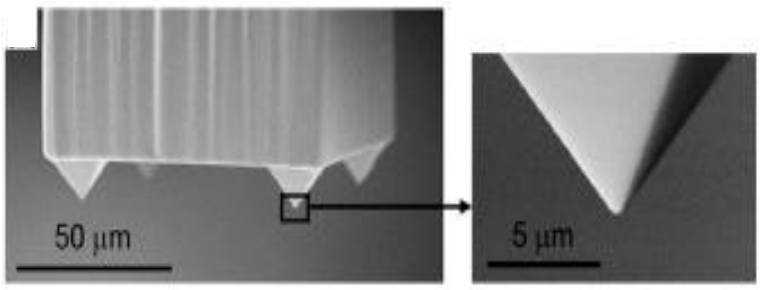

Figure 17.SEM picture of a microtip stamp fabricated in 5:1 PDMS. [7]

These pyramid stamps were fabricated in the following way. A 100 nm thick masking layer of SiN was patterned by plasma enhanced chemical vapor deposition (PECVD), followed by photolithographic patterning with SU-8 50 photocurable epoxy (MicroChem Corp.) on a Si [100] surface to make square pits, 15 um x 15 um, separated by 70 um, in a square packing arrangement. The exposed Si was then etched using an anisotropic KOH etch, with produced the pyramidal shaped pits, about 10.6 um deep. A second layer was then patterned over the pyramidal pits, so that when molded, the pits would protrude from the corners of a large pedestal. In this way, the potential adhesive strength of such a stamp is efficiently minimized. Not only is contact area between the stamp and the ink minimized, but the shapes of the tips themselves also facilitate lower adhesion. In the case of these pyramid stamps, the PDMS used was mixed in a 5:1 ratio of polymer to crosslinking catalyst. A stiffer material also facilitates a lower contact area in this design because the stiffer pyramid tips do not deform and flatten as much against the ink surface due to the attractive forces pressing them together. The actual contact area between the ink surface and each microtip can be quantified through calculation and finite element simulation. Classical contact mechanics tells us that the contact radius can be related to the microtip radius and the microtip cone angle, Θ, by a dimensionless function, S:

$$\frac{R_{\text{contact}}}{\gamma/\tilde{E}} = s\left(\frac{R_{\text{microtip}}}{\gamma/\tilde{E}}, \theta\right)$$

Where the interfacial tension is γ = 155 mJ/m^2, and the plain strain elastic modulus $\tilde{E}$ = E/(1-ν^2) = 2.4 MPa. Analysis shows that the contact radius decreases with the microtip

radius, but that it reaches an asymptotic value as the microtip radius approaches zero – which is to say, as the microtip becomes indefinitely sharp. This minimum value is described by the equation.

$$R_{\text{contact}}^{\min} = \frac{32\gamma}{\pi \bar{E}} \tan^2 \frac{\theta}{2}.$$

These methods of analysis put the contact radius between 680 to 732 nm, so the total contact area is easily under 1 um^2 per microtip.

The most novel function of this design – and the final feature discussed in this section – is tunable adhesion via roof collapse. Tunable adhesion is one of the major goals in the development of transfer printing technology. Tunable adhesion is the capability of a transfer printing stamp to have a very strong level of adhesion in one state, and weak adhesion in another. The stronger adhesive state is referred to alternately as the pick-up or inking state – that is to say, when the stamp lifts the ink from the donor substrate. The weaker adhesive state is referred to as the put-down or deposition state – that is to say, when the stamp leaves the ink on the target substrate. The functional criteria for the two states are simple: In the inking step, the adhesion between the ink and the stamp must be greater than the adhesion between the ink and the donor substrate. In the deposition step, the adhesion between the ink and the stamp must be weaker than the adhesion between the ink and the target substrate, but strong enough that the stamp will steadily hold on to the ink until it is deposited. Both of these modes are demonstrated in **figure 18.**

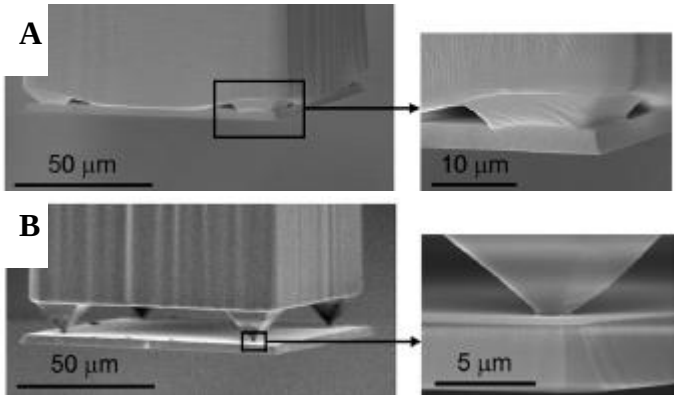

Figure 18. SEM image of microtip stamp in different modes of function. In the inking mode (A) the microtips and compressed and the roof is collapsed to maximize contact area. In the printing mode (B) only the tips of the pyramids are in contact with the ink square, so the minimized contact area facilitates deposition. [7]

Tunability in such devices can be either active or passive. Actively tunable adhesive stamps are devices in which the change in state is manually controlled by the user. Several technologies are currently in development to create transfer printing machines with active deposition mechanisms. Examples include elastomeric stamps with expanding bubble-shaped chambers and printing machines that assist deposition with the use of a highly focused laser. However, these are outside the scope of this thesis. Most of the designs we tested employed passively tunable adhesion, in which the stamp is designed to switch from one state to the other automatically. In the pyramid stamp design, this is achieved by taking advantage of the phenomenon of roof collapse, as described in the first section of this thesis, with the pyramids acting as the raised features, and the pedestal from which they were producing being the roof.

Roof collapse is a phenomenon that depends on the depth of the raised features, the stiffness of the material, and the attractive force between the material and the target substrate. It has three distinct regimes: stable, metastable, and unstable. In stable collapse, the roof collapses automatically without any extraneous force. The depth of the raised feature is small enough, the material soft and stretchable enough, and the dispersive attraction between the PDMS and substrate is great enough that such a collapse is highly favorable. In unstable collapse, the attractive forces are not enough to overcome the structural integrity of the microstructure, and only by the application of a mechanical normal force to the backing layer of the stamp is the roof forced to collapse. In this regime, once the normal force is removed, the stresses in the cured PDMS cause it to decollapse and return to its molded shape. In the metastable regime, the additional force is also necessary to cause collapse, however once that force is removed, the collapsed state remains. Decollapse can then be caused by creating some momentary stress in the material, thus encouraging it to return to the shape it was molded to be.

To achieve tunable adhesion via roof collapse, we constructed our stamps to behave at the intersection of the metastable and unstable regimes. This was facilitated by fabricating our stamp with consideration for the fact that each microtip had to have a certain minimum height, below which the elastic restoring force resulting from the stress in the deformed PDMS would not be sufficient to force decollapse. The equation describing this minimum height was found to be:

$$h_{\min} = \sqrt{\frac{w_{\text{stamp}}\gamma}{\bar{E}}\left[3.04\ln\left(\frac{w_{\text{stamp}}\bar{E}}{\gamma\tan^2\frac{\theta}{2}}\right) - 11.5\right]}$$

Where w_{stamp} was the width of the post (i.e. 100 um) and the angle $\Theta = 90^{o}$. In the collapsed state, contact area was maximized, and adhesion reducing features – in this case, the tapered shapes of the pyramids and their rounded tips – were essentially covered up, as the apparent contact area between the stamp and the ink were nearly 100%. The collapsed state was achieved by loading the stamp with a necessary normal load.

Once a good contact was made with the ink in this way, the stamp was rapidly retracted. The stress caused by the rapid retraction causes decollapse, so the important consideration for this step is simply to make the retraction happen quickly enough that decollapse does not occur before the ink is cleanly separated from its donor substrate. Once the ink has been transferred to the stamp – once the stamp has been "inked" – the stamp returns to its molded shape, in this case, with a set of pyramidal tips. In this way, the stamp is made to passively switch from its inking state to its deposition state, all while holding the ink square. Now, the adhesion between the stamp and the ink only needs to be strong enough for the stamp to be able to transport the ink to the target spot on the target substrate without dropping it, and if possible, without the ink shifting around on the stamp. If the ink shifts around on the stamp, it can still be easily deposited, but will have to be realigned when it is being brought down to the target substrate. Making certain that the adhesion is strong enough to hold the ink firmly will increase the throughput of this technology by eliminating the need for a corrective set of motions during the final

stages of the deposition step. Now the ink must simply be brought into contact with the target substrate without exerting additional strain on the stamp, so as not to cause it to collapse again, or if it does collapse, to allow for a relatively slow retraction so that decollapse occurs before the ink is separated from the target substrate. At this point, the features minimizing adhesion – most importantly, the minimal contact area – facilitate deposition.

Load cell data was thoroughly analyzed, taking into account several parameters with potential significance**.** In our methodology, a set of experiments with 1.5 millinewtons of preload and a set with 3 millinewtons of preload were performed. Both sets exhibited essentially the same behavior. The strength of adhesion was controlled by the rate of retraction of the stamp. As expected, the faster the pull-off rate, the greater the pull-off force When the pull-off rate exceeded a certain value – about 200 um/sec – the pull-off force reached an asymptote of about 0.6-0.8 millinewtons. When compared to the negligible pull-off forces associated with retraction that was slow enough that it did not take advantage of the collapsed roof, this shows a comparative increase of over a

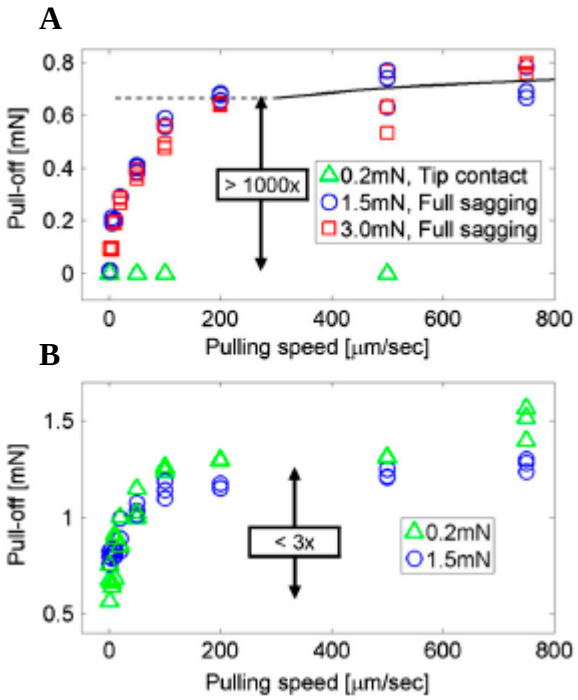

Figure 19. Plots of load cell data. The data for the structured PDMS stamp (A) demonstrates a 1000x increase of adhesion based on retraction velocity. An unstructured PDMS stamp was also tested to show a similar increase in adhesion of 3x due to viscoelastic effects. [7]

thousand-fold. This function is a result both of the engineered design of the stamp and of viscoelastic effects of the PDMS itself. Tot compare these effects specifically, a set of similar experiments was performed on an unstructured PDMS stamp of similar dimensions. The pull-off force showed a nearly identical dependence on retraction velocity, only in the absence of microstructures, the adhesion increase from a slow to a fast retraction velocity was only about threefold. This result, as represented by **figure 19**, shows both the ease with which viscoelastic effects can be coupled with motion control to facilitate tunable adhesion with any PDMS stamp design, as well as the enormous added benefit of a properly microstructured surface.

This is one of many possible designs for such a stamp. It is important to note the versatility of these geometrical features, as it is simple to change the exact form factor of each feature while retaining its basic function. For instnance, to minimize the total contact area even further, a pyramid microtip mold was fabricated with a fifth, larger pyramid in the center. Because of the stiffness of the ink samples we used, in this arrangement only three tips were ultimately in contact with the ink, as seen in **figure 20**. This versatility also enables us to integrate these features with one another, such as with spatula-shaped fibrillar surfaces that employ both contact splitting and stress redistribution effects, or in the case of our pyramid design, minimized contact area with tapered,

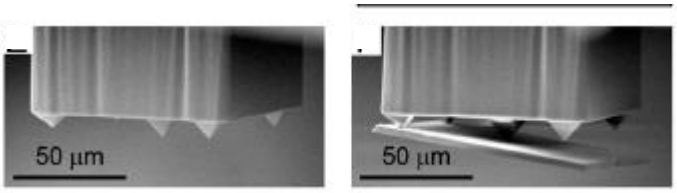

Figure 20. SEM image of alternative microtip design. The addition of a taller central pyramid maintains the same basic function described earlier, but further reduces contact in the printing mode from four microtips to three. [7]

rounded contact elements to minimize adhesion. Some features also present a much higher level of function when coupled with a proper motion. Tunability through roof collapse, is facilitated by controlling the rate of retraction, as controlled by the software running the printing machine.

Switchability of adhesion was demonstrably robust in our methodology. The 1000x difference in adhesive strength between inking and printing modes was encouraging not only because of the positive result of high adhesion in the inking mode, but because the extremely low adhesion in the printing mode enabled us to print our ink samples on several challenging substrates, and also in well-defined arrangements, as seen in **figure 21.**

The results reported above demonstrate that using a micropatterned surface in combination with specifically controlled motion results in an adhesive device with kinetically controlled switchability in its adhesive character. However, we also explored the possibility of kinetically controlled switchability of adhesive strength that was independent of any microstructural function. Although figure 19(B) shows such a result, kinetically varying normal motion was primarily seen as a means to the end of tuning adhesion via the roof collapse phenomenon. We also conducted a set of experiments exploring the effects of shear motion on the adhesive strength of unpatterned stamps.

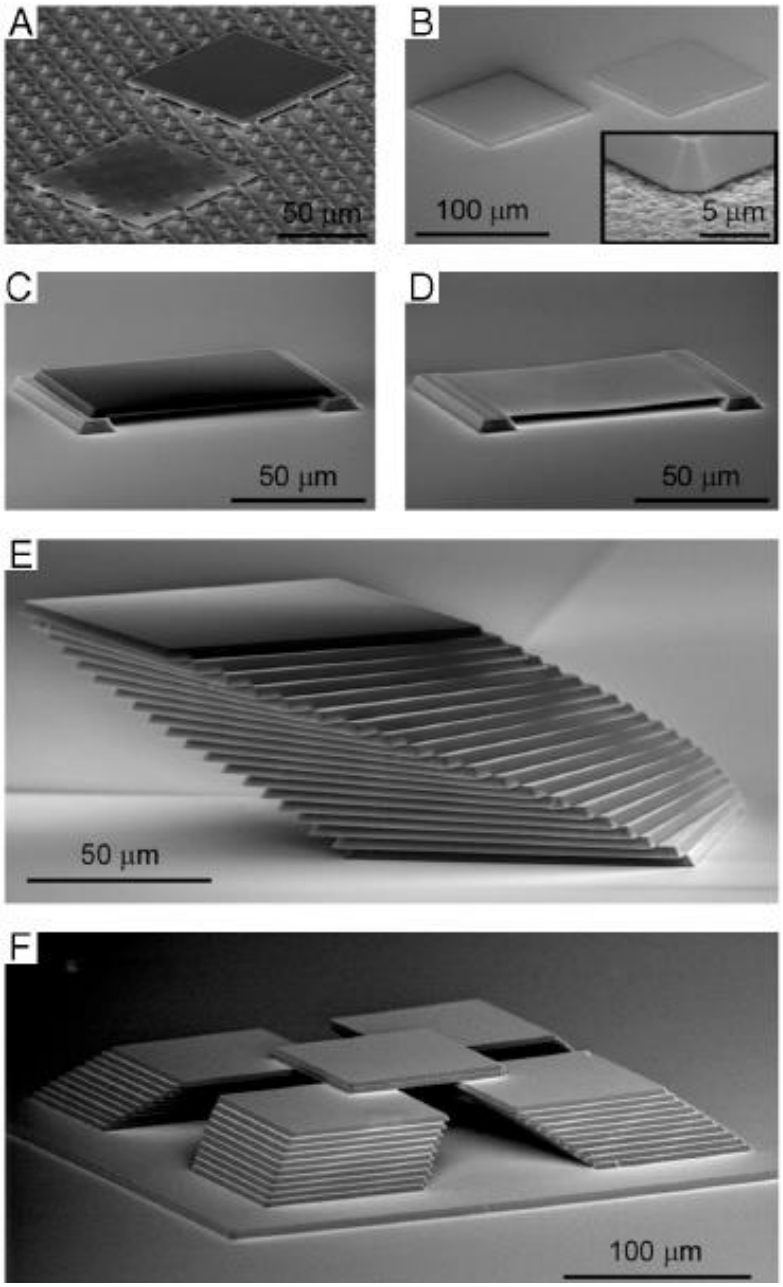

Figure 21. SEM images of printed Si ink samples on various surfaces and in controlled arrays. The microstructured transfer printing process was tested on thick (3 um) and thin (260 nm) Si platelets. The technique was robust for challenging printing surfaces such as a surface patterned with small square islands (A) and an ultrananocrystaline diamond surface (B) with an rms roughness >70 nm, as well as across two Si beams to create a suspended structure (C,D). The inks were also printed in multilayer configurations to show the robust control achievable with this technique (E,F). [7]

Shear stress effects were also considered**.** We predicted that a small shearing motion preceding normal retraction of an unpatterned PDMS post pressed against a smooth Si substrate would reduce the pull-off force associated with this retraction. We had already shown that if normal retraction was done at a high enough velocity, there would be a non-zero pull-off force due to viscoelastic effects. With this in mind, we designed a methodology to test our hypothesis which compared pull-off forces as measured by our 10 gram load cell for different amounts of shear. For completeness, we also ran these tests on stamps of several different aspect ratios, and found some interesting results. Our methodology was as follows: We fabricated several stamps of varying aspect ratios, from 1:1 – a cubic post – to 6:1 – a post with a large flat surface with a comparatively short post height. The post height was kept constant at 50 um for each sample, while the lateral dimensions of the post surfaces were varied from 50 to 300 um. Each stamp was tested by bringing it into contact with the substrate, preloading it with about 3 mN of force, and then giving it a 5 second dwell time for relaxation, as with all previous experiments. The automated program controlling the transfer printer then had the horizontally articulating stage move a small amount in one direction, followed immediately by a rapid retraction. The amount of shear motion was divided into increments of percent shear strain, which we defined as the ratio of shear motion to the vertical dimension of the post. Each set of shearing experiments was performed twice for each stamp – once at a retraction velocity of 10 um/s and once at a retraction velocity of 1000 um/s.

First, shear motion did in fact drive down the pull-off force, as predicted. The greater the amount of shear motion experienced by the stamp before pull-off, the lower

the pull-off force registered by the load cell. This is evident by the general downward trend of the plots in **figure 22**. The difference between the two retraction velocities were also expected, based on the viscoelastic effect and its dependence on pull-off rate shown in figure 19(B). The pull-off forces were always greater when the pull-off velocity was 1000 um/s than when it was only 10 um/s.

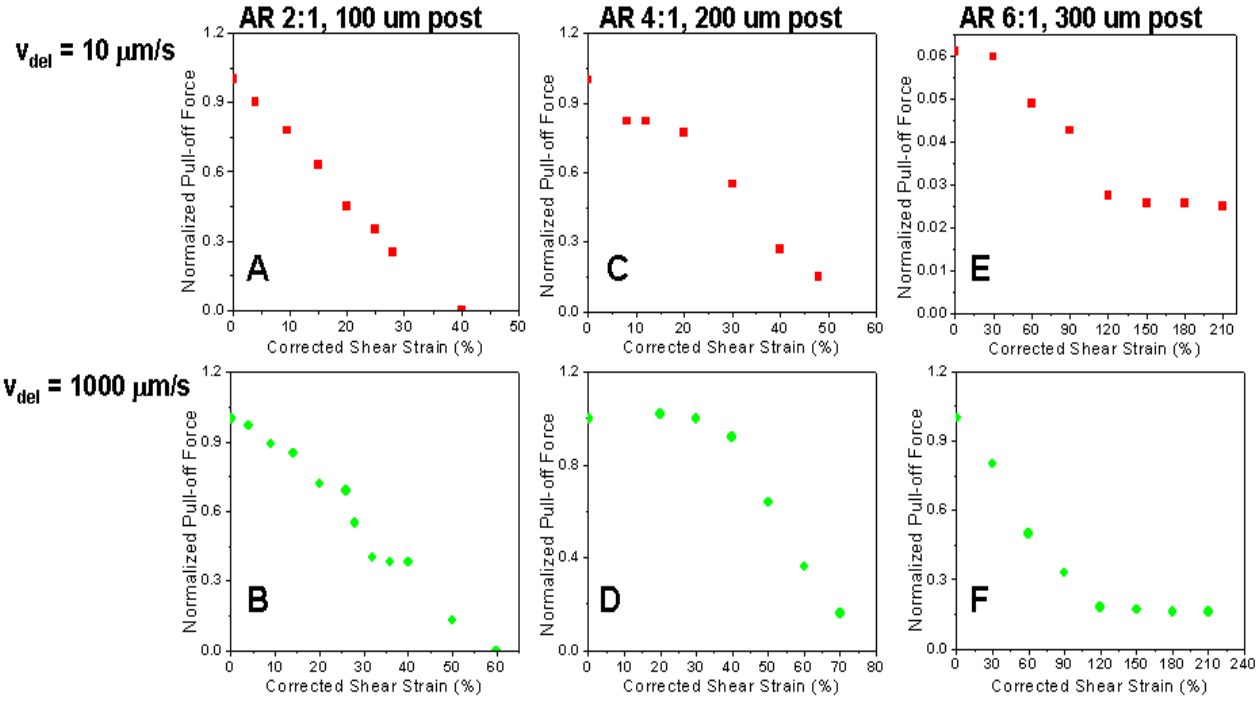

Figure 22. Plots of shear strain vs. pull-off force for unstructured PDMS posts. Experiments were performed to quantify the effects of shear stress on the adhesive strength of PDMS posts of varying aspect ratios and at two different pull-off velocities. These plots show the fact that shear motion drives down pull-off force, while higher aspect ratios increase it, as does increased pull-off velocity.

In addition to these results, we also observed some interesting phenomena that can be summarily described as dragging and slipping. As the post was sheared, the contact area waned in way described by figure 12(B). However, after a critical distance of shear motion, a critical contact area would be reached, and this contact area would drag along the substrate surface. The critical shear distance at which this behavior began depended on the dimensions of the post – the wider the contact surface, i.e. the higher the aspect ratio, the sooner the critical contact area was reached. Moreover, the dragging of the critical contact area would occur in two different ways: Either the contact area would drag smoothly across the substrate surface, or it would rapidly shift back and forth, skidding across the surface. These phenomena also seemed to depend on the aspect ratio of the posts, although this dependence was not conclusive from our data. Their occurrence was evident both through visual verification, and they were detectable by the load cell. The load cell's response to such shear motion is shown in **figure 23**. As the post was sheared across the substrate, PDMS material began to bunch up at the leading edge of the contact area, causing a build up of material their that pushed the load cell downward, and thus causing the load cell to register shear motion as an increase in the normal downward force. If the critical area dragged smoothly across the substrate, the load cell would register a flat level for that time span. However, if slipping occurred, the load cell registered periodic spikes with each skidding/slipping event.

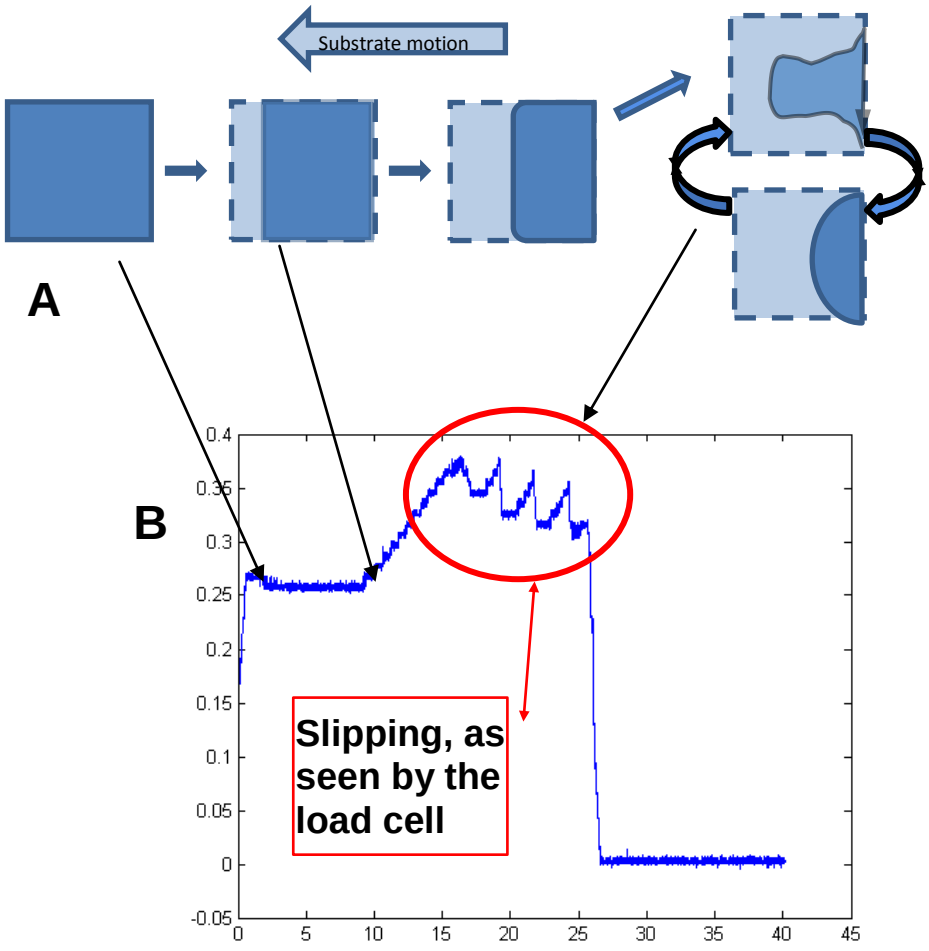

Figure 23. Slipping of contact area during shear as seen through optics (A) and by the load cell (B). A visual schematic (A) provides a time line of events as the post is being sheared to the right across the substrate. In practice, it is the substrate that is mounted on the horizontally articulating stage, so substrate motion is denoted as being toward the left. The light square represents the total post area, while the waning dark rectangle represents the changing contact area between the post and the Si substrate. In slipping, the final contact area switches rapidly between a hemispherical shape and some other random shape, and this is detected by the load cell as a series of spikes (B). In smooth dragging, the final contact area remains hemispherical and the load cell plot reaches an asymptotic maximum.

The most interesting aspect of this observation was the fact that it seemed to correlate with a plateau in the adhesion data, most evident in the plots described in figure 22(E,F). For certain aspect ratios, after a certain critical shear distance had been reached, the pull-off force remained the same. Additional shear motion no longer drove down the adhesive strength of the posts. The exact parameters of this plateau seemed to be correlated with the dimensions of each particular post, but the precise nature of the relationship was not conclusive from our data. The fact that the appearance of the plateau in adhesive strength coincided with the approach of a critical contact area led us to postulate that the two are related. One likely conclusion is that the waning contact area is one of, if not the main cause of reduced adhesion in the presence of shear motion, and therefore, that once the contact area has been maximally reduced, so has the adhesion. To properly test this hypothesis and thoroughly quantify the interdependence of these effects, more experiments would be needed.

CHAPTER 7

CONCLUSIONS AND FUTURE WORK

The need for simple, clean, and efficient fabrication techniques and evidence of highly effective dry adhesion in natural systems led us to explore the possibilities of bioinspired adhesive devices that would be able to manipulate nanoscale objects for a variety of uses. Because biological systems such as insects, geckos, and even pollen particles demonstrated an ability to adhere to almost any surface without the use of messy chemicals to facilitate this adhesion, such systems were of particular interest, and were researched at length. The background research suggested that so long as the surfaces in question were not very weakly polarizable, van der Waals forces, aka dispersive bonding would present very effective adhesion on the nano scale. The reason that these forces are so much more effective on the nano scale than on a macro scale is simply the fact that these forces act over very small distances, and so if the contacting area is measured in nanometers rather than centimeters, surface roughness is less likely to interfere with the necessary contact. In short, a more intimate contact was all that was necessary to take advantage of these intermolecular attractions, and this was achieved in part automatically by virtue of the scale we desired work on, and was also helped by the use of soft PDMS which would conform to some degree to any surface it was contacting.

Once we understood this, we set out to test two categories of parameters: microstructure and motion. For the former, we identified several types of features – mostly from biomimetic inspiration, but also in some cases from established engineering principles – that affected the adhesive behavior at an interface. For the latter, we

performed tests on both patterned and unpatterned surfaces that showed that different rates and modes of motion had significant, quantifiable effects on the adhesive character of the interfaces in question.

We report positive results on both fronts, most notably on the robustness of microstructured surfaces that are engineered to have specific properties and behaviors. Simply by adding posts to the surface of a stamp, we were able to passively switch adhesion between a strong and a weak mode by manipulating the phenomenon of roof collapse. By controlling the height of the added surface features we were able to control the switching of the two modes which depended on the maximized contact area of the collapsed state for stronger adhesion. By making the features pyramidal so that they would terminate in a microtip we minimized the contact area in the uncollpased state, thus driving adhesion in the weak mode down to a negligibly small magnitude.

Furthermore, we report that there are many advantages associated with paying special attention to the transfer printing motions themselves. Rate of motion, especially in the normal pulling direction greatly affects the maximum force necessary to break the interface between a PDMS stamp and a smooth Si substrate. Shear motion also exhibits some interesting effects that can be summarized as a general reduction of adhesive strength at the interface.

In the area of kinetic control of adhesive character, there are many possible directions for further exploration. We observed a plateau in the adhesion-reducing effects of simple lateral shear motion which warrants further study for proper quantification. There are also many other methodologies that may produce interesting results, both in

more detailed study of the effects of rate of motion (eg rates of different types of motion or rates of varying steps of motion within a given cycle), as well as more possible modes of motion (eg rotational shear). In addition to these simple experiments – which should be initially performed on unstructured posts – methodologies that combine some physical form factor that is designed to be used with a specific mode of motion are limited only by the designer's imagination.

We also discussed some physical features with potentially useful effects that were not part of our primary experiments, such as vacuum chambers, contact splitting, stress redistribution, and crack arresting features. These features may be useful for a given application and should be considered a part of the suite of tools being developed by researchers studying adhesive mechanics of microstructured surfaces and interfaces. Other physical features with interesting and useful functions are also possible to invent, and again are limited only by the inventor's imagination.

Future directions for related research can be divided into two categories: method development and device innovation. Method development, which is what this thesis primarily deals with, refers to research that grows the base of knowledge required for the techniques I have described. In order for progress to be made on this front, researchers must build upon the basic understanding of how methodology, surface chemistry and geometry affect the strength of a given interface. Goals for this sort of research should include verifying physical phenomena with robust modeling, further exploration of basic design details and their effect on printing function, and generally any goal that helps to fill out the parameter space associated with technique, such as size limitations, effects of

motion rate, and dimensional proportions that optimize function.

Once the underlying principles of transfer printing technology are established to the point that it becomes an economically viable fabrication method, there will be a much greater demand for ideas on how to use this technology. Device innovation is increasingly an important direction for future researchers to progress in. As the capability to print novel devices on novel substrates increases, researchers – particularly those with interdisciplinary backgrounds – will seek new ways to integrate electronic components. More effective bio-sensors will become more feasible, as will devices such as better pacemakers. Even the fact that this method would allow for digital displays to be placed in more creative and versatile ways is very promising. Device innovation is a future direction for research that almost any person working with consumer technology can contribute to, once the true effectiveness of this technique can be established.

Ultimately, we demonstrated the ability of microstructured PDMS stamps to maximize adhesion – meaning that most any ink can likely be retrieved, either with the simple system we tested on the transfer printer, or with the addition of other interface strengthening features as may be needed – and also to minimize adhesion, which is in some ways the most useful aspect of this technology.

By having an inked stamp that is steadily but very weakly holding on to its ink, we can guarantee deposition on a wide variety of challenging target surfaces. Aside from allowing the user to build sophisticated structures with great dexterity, this capability potentially opens up a whole new class of electronic devices, as semiconductor chips can

now be printed on substrates where electronic devices could not previously be fabricated. This means that electronic device fabrication can be untethered from the rigid plain of existence on which it was developed. Electronic devices can be fabricated on elastic, curvilinear substrates, enabling new form factors and thus a whole new world of uses. The ability to assemble electronic devices directly on existing functional surfaces is also an area of great potential. Transfer printing can potentially be used for the assembly of electronic devices on anything from paper to skin.

The demands and limitations of the fabrication processes which we seek to replace have also been discussed at length in this thesis, as they are the primary methods we used to fabricate our own samples. It is our hope that transfer printing technology will someday replace the messy, complicated, and overall difficult methods currently used to fabricate nanoelectromechanical systems, as well as to enable nanotechnologists to assemble those systems however and wherever they would be most useful.

REFERENCES

1. Imbaby, M.F. and K. Jiang, *Fabrication of free standing 316-L stainless steel-Al2O3 composite micro machine parts by soft moulding.* Acta Materialia, 2009.
2. Arzt, E., S. Gorb, and R. Spolenak, *From micro to nano contacts in biological attachment devices.* Proceedings of the National Academy of Sciences, 2003(100): p. 10603-10606.
3. Huang, Y.Y., et al., *Stamp Collapse in Soft Lithography.* Langmuir, 2005. **21**: p. 8058-68.
4. Feng, X., et al., *Competing Fracture in Kinetically Controlled Transfer Printing.* Langmuir, 2007. **23**(25): p. 12555.
5. Boesel, L.F., et al., *Gecko-Inspired Surfaces: A Path to Strong and Reversible Dry Adhesives.* Advanced Materials, 2010. **22**: p. 2125-2137.
6. Gantz, K., L. Renaghan, and M. Agah, *Development of a comprehensive model for RIE-lag-based three-dimensional microchannel fabrication.* Journal of Micromechanics and Microengineering.
7. Kim, S., et al., *Microstructured elastomeric surfaces with reversible adhesion and examples of their use in deterministic assembly by transfer printing.* Proceedings of the National Academy of Sciences, 2010. **107**(40): p. 17095-17100.
8. Israelachvili, J.N., *Intermolecular and Surface Forces*. Vol. chap 15. 1985, New York: Academic Press.
9. Kendall, K., *Adhesion: Molecules and Mechanics.* Science, 1994. **263**: p. 1720-.

10. Chaudhury, M.K., *Interfacial interaction between low-energy surfaces.* Materials Sciences and Engineering, 1996. **R16**: p. 97-159.

11. Maeda, N., et al., *Adhesion and Friction Mechanisms of Polymer-on-Polymer Surfaces.* Science, 2002. **297**(5580): p. 379.

12. Vilmin, T., et al., *Interdigitation between surface-anchored polymer chains and an elastomer: Consequences for adhesion promotion.* EPL (Europhysics Letters), 2004. **68**: p. 543.

13. London, F., *The General Theory of Molecular Forces.* 1936.

14. Derjaguin, B.V., Y.I. Rabinovich, and N.V. Churaev, *Direct measurement of molecular forces.* Nature, 1978. **272**(5651): p. 313.

15. Tabor, D. and R.H. Winterton, *Surface forces: direct measurement of normal and retarded van der Waals forces.* Nature, 1968. **219**: p. 1120-1.

16. Tadmor, R., *The London-van der Waals interaction energy between objects of various geometries.* Journal of Physics: Condensed Matter, 2001. **13**: p. L195-L202.

17. Hsiaa, K.J., et al., *Collapse of stamps for soft lithography due to interfacial adhesion.* APPLIED PHYSICS LETTERS, 2005. **86**: p. 154106.

18. Newby, B.Z., *Microscopic Evidence of the Effect of Interfacial Slippage on Adhesion.* Science, 1995. **269**: p. 1407.

19. Holl, S.M., et al., *Solid-State NMR Analysis of Cross-Linking in Mussel Protein Glue.* Archives of Biochemistry and Biophysics, 1993. **302**: p. 255-258.

20. Skordos, A., et al., *A novel strain sensor based on the campaniform sensillum of insects.* Philos Transact A Math Phys Eng Sci., 2002. **360**: p. 239-53.

21. Lamblet, M., et al., *Adhesion Enhancement through Micropatterning at Polydimethylsiloxane−Acrylic Adhesive Interfaces.* Langmuir, 2007. **23**: p. 6966-6974.

22. Vincent, J.F.V. and D.L. Mann, *Systematic technology transfer from biology to engineering.* Phil. R. Trans. Soc. London, 2002. **360**: p. 159-173.

23. Autumn, K., et al., *Evidence for van der Waals adhesion in gecko setae.* Proc Natl Acad Sci U S A., 2002. **99**: p. 12252-6.

24. Autumn, K. and A.M. Peattie, *Mechanisms of Adhesion in Geckos.* Integrative and Comparative Biology, 2002. **42**: p. 1081-1090.

25. Federle, W., et al., *Biomechanics of the movable pretarsal adhesive organ in ants and bees.* Proceedings of the National Academy of Sciences of the United States of America, 2001. **98**(11): p. 6215-6220.

26. Federle, W., et al., *Wet but not slippery: boundary friction in tree frog adhesive toe pads.* Journal of The Royal Society Interface, 2006. **3**(10): p. 689-697.

27. Bellairs, A., *The Life of Reptiles*. 1970: Universe Books, New York.

28. Autumn, K., et al., *Adhesive force of a single gecko foot-hair.* Nature, 2000. **405**(6787): p. 681.

29. Chui, B.W., et al., *Independent detection of vertical and lateral forces with a sidewall-implanted dual-axis piezoresistive cantilever.* Appl. Phys. Lett., 1998. **72**: p. 1388-1390.

30. Irschick, D.J., et al., *A comparative analysis of clinging ability among pad-bearing lizards.* Biol. J. Linn. Soc, 1996. **59**: p. 21-35.

31. Johnson, K.L., K. Kendall, and A.D. Roberts, *Surface energy and the contact of*

elastic solids. Proceedings of the Royal Society of London, 1971. **324**: p. 301-313.

32. Kamperman, M., et al., *Functional Adhesive Surfaces with ''Gecko'' Effect: The Concept of Contact Splitting.* ADVANCED ENGINEERING MATERIALS, 2010. **12**: p. 335-348.

33. Persson, B.N.J., *On the mechanism of adhesion in biological systems.* The Journal of Chemical Physics, 2003. **118**: p. 7614-22.

34. Chen, B., P.D. Wu, and H. Gao, *Hierarchical modelling of attachment and detachment mechanisms of gecko toe adhesion.* Proc. R. Soc. A, 2008. **464**: p. 1639-1652.

35. Hur, S.-H., et al., *Nanotransfer printing by use of noncovalent surface forces: Applications to thin-film transistors that use single-walled carbon nanotube networks and semiconducting polymers.* Applied Physics Letters, 2004. **85**: p. 5730-5732.

36. Rogers, J.A., *Electronics: A Diverse Printed Future.* Nature, 2010. **468**.

37. Liu, C.X. and J.W. Choi, *Patterning conductive PDMS nanocomposite in an elastomer using microcontact printing.* Journal of Micromechanics and Microengineering, 2009. **19**.

38. Bennett, R.D., et al., *Creating Patterned Carbon Nanotube Catalysts through the Microcontact Printing of Block Copolymer Micellar Thin Films.* Langmuir, 2006. **22**(20): p. 8273.

39. Ling, Z., C. Liu, and K. Lian, *Design and fabrication of SU-8 micro optic fiber holder with cantilever-type elastic microclips.* Microsystem Technologies, 2009.

15: p. 429-35.

40. Rizzo, A., et al., *Hybrid Light-Emitting Diodes from Microcontact-Printing Double-Transfer of Colloidal Semiconductor CdSe/ZnS Quantum Dots onto Organic Layers.* Advanced Materials, 2008. **20**(10): p. 1886.

41. Park, S.-I., et al., *Printed Assemblies of Inorganic Light-Emitting Diodes for Deformable and Semitransparent Displays.* Science, 2009. **325**: p. 977-981.

42. Feigl'man, M.V., M.A. Skvortsov, and K.S. Tikhonov, *Theory of proximity-induced superconductivity in graphene.* Solid State Communications, 2009. **149**: p. 1101-05.

43. Shaw, K.A., Z.L. Zhang, and N.C. MacDonald, *SCREAM I: a single mask, single-crystal silicon, reactive ion etching process for microelectromechanical structures.* Sensors and Actuators A, 1994. **40**: p. 63-70.

44. Liao, Y.Y. and J.H. Liu, *Preparation and characterization of molecular photoresists: Crosslinkable positive and water developable negative tones.* Journal of Applied Polymer Science, 2008. **109**: p. 3849-58.

45. Kim, D.-H., et al., *Complementary Logic Gates and Ring Oscillators on Plastic Substrates by Use of Printed Ribbons of Single-Crystalline Silicon.* IEEE Electron Device Letters, 2008. **29**: p. 73 - 76.

46. Kim, T.-H., et al., *Kinetically Controlled, Adhesiveless Transfer Printing Using Microstructured Stamps.* Applied Physics Letters, 2009. **94**: p. 113502.

47. Siegel, A.C., et al., *Cofabrication: A Strategy for Building Multicomponent Microsystems.* Accounts of Chemical Research. **43**(4): p. 518.

48. Rogers, J.A. and U. Paik, *Nanofabrication: Nanoscale Printing Simplified.*

Nature Nanotechnology, 2010. **5**: p. 285-386.

49. Lötters, J.C., et al., *The mechanical properties of the rubber elastic polymer polydimethylsiloxane for sensor applications.* Journal of Micromechanics and Microengineering, 1997. **7**: p. 145.

50. Loo, Y.-L., et al., *High-Resolution Transfer Printing on GaAs Surfaces Using Alkane Dithiol Self-Assembled Monolayers.* Journal of Vacuum Science and Technology B, 2002. **20**: p. 2853-2856.

51. Meitl, M.A., et al., *Transfer printing by kinetic control of adhesion to an elastomeric stamp.* Nat Mater, 2006. **5**(1): p. 33.

52. Love, J.C., et al., *Self-Assembled Monolayers of Thiolates on Metals as a Form of Nanotechnology.* Chemical Reviews, 2005. **105**(4): p. 1103.

53. Johannes G., V., R.J. Forster, and T.E. Keyes, *Interfacial Supramolecular Assemblies.* Vol. pp. 88–94. 2003: Wiley.

54. Lee, H.H., et al., *Fabrication of large-area stamps, moulds, and conformable photomasks for soft lithography.* Proceedings of the Institution of Mechanical Engineers, Part N: Journal of Nanoengineering and Nanosystems, 2004. **218**: p. 1-5.

55. Lee, G., et al., *High-Throughput Synthesis and Measurement Methods for Rapid Optimization and Discovery of Advanced Materials.* Materials Research Society Symposium Proceedings, 2009. **1159**: p. 25-30.

56. Shull, K.R., et al., *Axisymmetric Adhesion Tests of Soft Materials.* Macromol. Chem. and Phys, 1998. **199**: p. 489.

57. Meitl, Matthew Alexander, *Transfer Printing and Micro-Scale Hybrid Materials*

Systems : 2007. Print.